

# Vaisala Xweather Solar Model 3 database

Methodology and  
validation - 2025

# Table of contents

<b>1 Introduction</b>	3
1.1 Solar terminology and parameters	5
1.2 Ground measurements vs satellite-based models	5
1.3 Solar development roadmap	6
1.3.1 Prospecting and planning	6
1.3.2 Design and due diligence	6
1.4 Vaisala Xweather Solar Model 3: Products	7
<b>2 xweather renewable energy solar irradiation database</b>	8
2.1 Spatial and temporal coverage	10
2.2 Key features	11
2.3 Description of the Heliosat-V method	11
2.3.1 Heliosat-V cloud-index computation	13
2.3.2 The clear-sky reflectances pclear	14
2.3.3 The overcast-sky reflectances pocc	15
2.3.4 McClear clear-sky model	16
2.3.5 Inputs (cloud-index part)	16
2.3.6 Inputs (clear-sky part)	16
2.3.7 Sources of errors in GHI computation	17
2.4 Post-processing	18
<b>3 Validation</b>	19
3.1 Definition of the indicators	20
3.2 Measurements	20
3.3 Quality check	21
3.4 Validation across Meteosat field of view	22
3.4.1 List of measurement stations	22
3.4.2 Global statistics	24
3.5 Validation across GOES East field of view	26
3.5.1 List of measurement stations	26
3.5.2 Global statistics	27
3.6 Validation across GOES West field of view	29
3.6.1 List of measurement stations	29
3.6.2 Global statistics	30
3.7 Comparison with other solar databases	32
<b>4 Conclusion and perspectives</b>	33
<b>5 Annex</b>	35
5.1 Statistics per station	36
5.1.1 Meteosat	36
5.1.2 GOES East	38
5.1.3 GOES West	38
5.2 Acronyms	39
5.3 Glossary	40
5.4 References	41

# Introduction





Solar energy production is directly correlated to the amount of radiation received at a project location.

Like all weather-driven renewable resources, solar radiation can vary rapidly over time and space, and understanding this variability is crucial in determining the financial viability of a solar energy project.

The three components of irradiance most critical for determining solar installation production values are global horizontal irradiance (GHI), direct normal irradiance (DNI), and diffuse horizontal irradiance (DIF). In this paper we are focused on validating GHI, or the total amount of radiation received by a horizontal surface, which is the primary resource in photovoltaic (PV) installations.

Different approaches already exist to produce such GHI data. Sources of data mainly include ground pyranometric measurements, numerical weather prediction modeling, and satellite-based remote sensing [Sengupta 2021]. Satellite-based methods are an efficient and accurate way to produce kilometric and sub-hourly resolved multidecadal time series of GHI. A more comprehensive review of pros and cons of different methods is notably described in [Huang 2019].

The Vaisala Xweather Solar Model 3 uses the Heliosat-V method [Tournadre 2020]. Heliosat-V is a new way of retrieving the GHI from a large variety of satellite instruments sensitive to reflected solar radiation, embedded on geostationary satellites. Heliosat-V is

part of the family of "cloud index" methods. The cloud index is a widely used proxy for the effective cloud transmissivity. To reach its versatility, the method uses simulations from a fast radiative transfer model to estimate overcast (cloudy) and clear-sky (cloud-free) satellite scenes of the Earth's reflectances. Simulations consider the anisotropy of the reflectances caused by both surface and atmosphere and are adapted to the spectral sensitivity of the sensor. The anisotropy of ground reflectances is described by a bidirectional reflectance distribution function model and external satellite-derived data.

The XweatherSolar Model 3 database is currently generated from Meteosat 0°, GOES East and GOES West satellites imagery. It has been compared to 87 locations where high-quality in situ measurements of GHI are available from the Baseline Surface Radiation Network (BSRN), the EnerMENA Meteorological Network in the MENA Region, the validation dataset of the IEA PVPS, the Energy Sector Management Assistance Program (ESMAP), the SAURAN national program in South Africa and the Brazilian National Institute for Space Research INPE.

In average, results from the Xweather solar model 3 and ground-based measurements show a mean bias error (MBE) of 0.36% to 0.86% (depending on the satellite), a bias standard deviation of 1.34% to 2.72%, an hourly mean absolute error (MAE) of 8.32 to 11.11% and an hourly root mean square error (RMSE) of 13.39 to 17.48%.

## 1.1 Solar terminology and parameters

Solar resource availability determines how much electricity will be generated in a given time. Analysis of the solar radiation components makes it possible to understand the performance of solar power plants.

From the terminology point of view, it is to be noted

that while solar irradiance refers to solar power (instantaneous energy) falling on a unit area per unit time [W/m<sup>2</sup>], solar irradiation is the amount of solar energy falling on a unit area over the given time interval [Wh/m<sup>2</sup> or kWh/m<sup>2</sup>]. To avoid confusions, the Xweather Solar Model 3 offers only solar irradiation.

Solar resource components provided by the Xweather solar model 3:

Component	Acronym	Description	Unit
Global horizontal irradiation	GHI	Total irradiation that reaches the surface (on a horizontal plane). It is considered as the reference component.	Wh/m <sup>2</sup> or kWh/m <sup>2</sup>
Direct normal irradiation	DNI	Component that directly reaches the surface. It is relevant for concentrating solar thermal power plants (CSP).	
Diffuse horizontal irradiation	DIF	Part of the irradiance that is scattered by the atmosphere.	
Global tilted irradiation	GTI	Total irradiation that reaches a tilted surface. It is relevant for photovoltaic (PV) technology.	

## 1.2 Ground measurements vs satellite-based models

Most financing options for solar projects require information on expected yearly irradiance values as projects typically must service debt one to four times per year. However, annual averages do not provide enough information to determine accurate annual irradiance and power production values.

Depending on the characteristics of a site, studies have shown that on average, annual irradiance means can differ from the long-term mean by 5% for GHI and by as much as 20% for DNI. Thus, a long-term record of solar irradiance estimates is needed to calculate a realistic variance of production values.

High-quality solar resource and meteorological data is available today, and it can be obtained by 3 approaches:

- High-quality solar instruments at meteorological stations: Well-maintained ground-based instruments provide high-accuracy, high-frequency data for specific locations. However, the global network of surface stations is sparse and often lacks long-term data, with many stations offering only short-term records (ranging from months to a few years). These stations are rarely located near proposed project sites and are prone to measurement errors if not properly maintained. Common issues include dirty sensors, misalignment, miscalibration, data logger faults, and other operational failures.
- Numerical Weather Prediction (NWP) models: These models offer global coverage and are generally robust, but they have limited spatial and temporal

resolution (e.g., 9 km and 1 hour for ECMWF's IFS model), which can affect accuracy for localized solar resource assessments.

- **Satellite-based solar models:** These models use satellite imagery along with atmospheric and meteorological data to estimate solar radiation. While typically less accurate than high-quality ground measurements, they provide consistent,

long-term coverage (often exceeding 20 years) for virtually any location. Satellite-derived data is stable and not subject to the operational issues of ground stations. In fact, for locations more than 25 km from a surface station, satellite estimates are often more accurate than the nearest ground-based observations.

## 1.3 Solar development roadmap

Developing a solar project requires a large upfront investment. A standard development roadmap conserves time and money and ensures that the most promising projects are constructed. Each stage of development asks different questions about the solar resource and each stage requires varying degrees of information and financial investment.

### 1.3.1 Prospecting and planning

The first step in building any solar energy project is identifying the locations most suitable for development. The price of energy, access to transmission, and environmental siting issues should all be taken into consideration, but the most essential variable is the availability of the solar resource – the “fuel” of the project. At this early stage, average annual and monthly solar irradiance values can be used to assess the overall feasibility of a particular site and to select the appropriate solar technology to be installed. Getting time series or typical meteorological year (TMY) data is an even better method.

Note: Vaisala plans to provide TMYs using the Vaisala Xweather solar model 3 in Q1 2026.

### 1.3.2 Design and due diligence

Once a promising site is identified, a more in-depth analysis is required to better quantify the long-term availability of the solar resource, to design technical aspects of the project, and to secure the upfront capital for construction. A common source of solar data used for this purpose is TMY data. A TMY dataset provides a 1-year, hourly record of typical solar irradiance and meteorological values for a specific location in a simple file format. Although not designed to show extremes, TMY datasets are based on a long time period and show seasonal variability and typical climatic conditions at a

site. They are often used as an input to estimate average annual energy production.

While TMY data provide a good estimate of the average solar irradiance at a site, they are not a good indicator of conditions over the next year, or even the next 5 years. The U.S. National Renewable Energy Laboratory User Manual for TMY3 data explicitly states, “TMY should not be used to predict weather for a particular period of time, nor are they an appropriate basis for evaluating realtime energy production or efficiencies for building design applications or a solar conversion system.”<sup>4</sup> Hourly time series covering a period of several years provide a much more complete record for calculating accurate estimates of solar resource variability.

Year-to-year variability has a significant impact on annual energy production. Many financial and rating institutions, as well as internal certification organizations, require 1-year P90 values to assess

the economic feasibility of a project. A 1-year P90 energy value indicates the production value that the annual energy output will exceed 90% of the time. A 1-year P90 value (as opposed to a 10-year P90 value) is typically mandatory because most solar projects have a lending structure that requires them to service debt one to four times a year, not one to four times every 10 years. If power production decreases significantly in a given year due to solar variability, debt on the project may not be able to be paid and the project could default on its loan. This is precisely what financiers are trying to avoid. The only way to determine 1-year P90 values acceptable to funding institutions is with long-term continuous data at the proposed site.

## 1.4 Vaisala Xweather Solar Model 3 products

With Xweather's latest offering, making informed decisions has never been easier. This advanced, satellite-based data set delivers the reliable, high-accuracy information you need to optimize every phase of your solar project.

Discover Xweather's next-generation irradiation model, now available through two new products designed to address the key challenges of modern solar energy applications:

- **Xweather Solar Model 3 Archive Data:** Access decades of high-precision solar irradiation data to accurately size and benchmark your projects with unmatched historical insight.
- **Xweather Solar Model 3 Monitoring Data:** Gain high accuracy, near real-time solar irradiation data to empower your O&M teams. Instantly detect underperformance, identify soiling issues, and benchmark energy output against actual solar input with ease.



# Vaisala Xweather Solar Model 3 database

2

As discussed earlier in this document, satellite-derived data have proven to be the most accurate method of estimating surface solar irradiance beyond 25 km of a ground station. However, either technology requires special consideration.

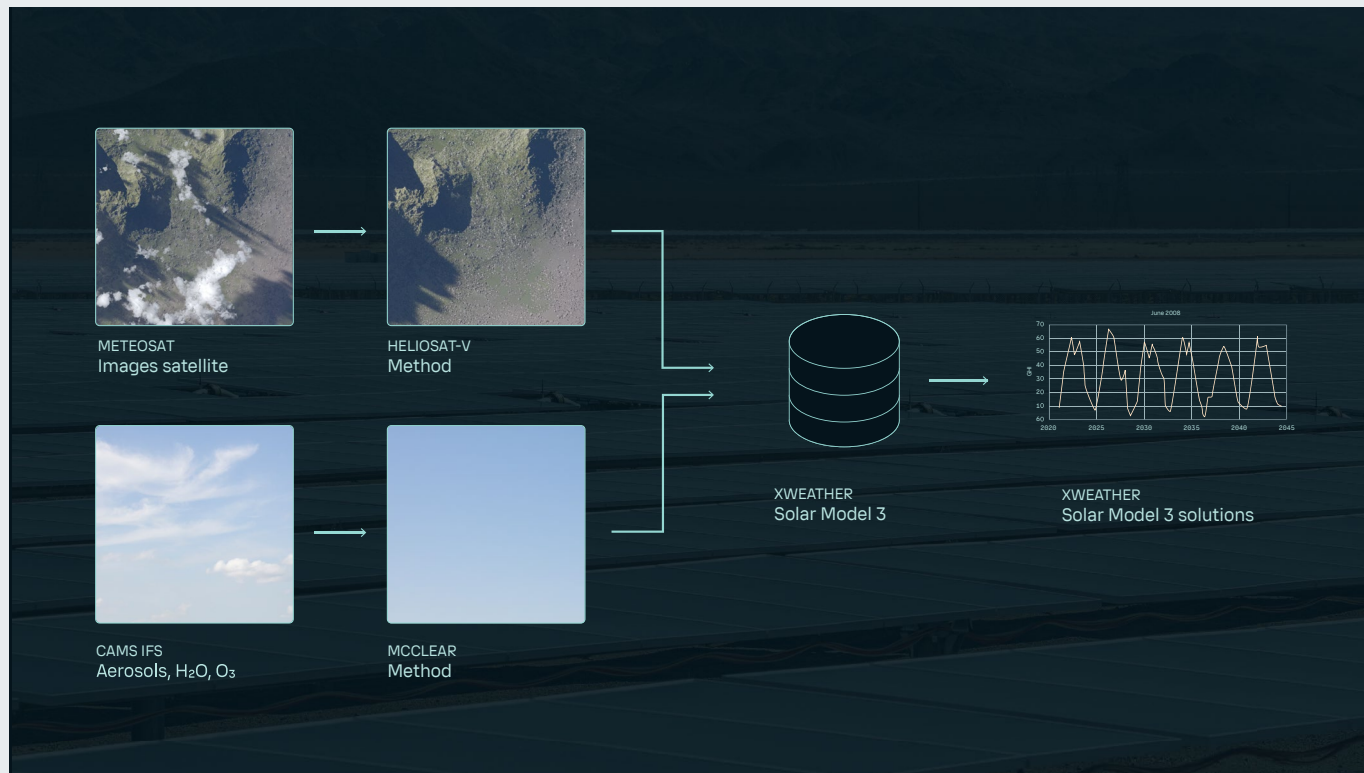
For example, if there is a dramatic elevation difference between a ground station and a project location, data from the ground station may not be representative of conditions at the project site. Satellite data accuracy can also be influenced by local terrain, such as in locations along coastlines or near dry lake beds.

Vaisala's main source of satellite observations is weather satellites in a geostationary orbit. These satellites have the same orbital period as the Earth's rotation and are thus stationary relative to a point on the earth. As a result, their instruments can make multiple observations of the same area with identical viewing geometry. Vaisala's methodology uses visible satellite imagery to calculate the level of cloudiness at the Earth's surface. The resulting time series of cloudiness (or cloud index)

is then combined with other information to model the amount of solar radiation at the Earth's surface. The outcome is a 20+ year dataset that provides hourly and sub-hourly estimates of surface irradiance (GHI, DNI, and DIF).

Vaisala's global solar dataset is based on two decades of sub-hourly high-resolution visible satellite imagery via the broadband visible wavelength channel. These data have been processed using a combination of peer-reviewed, industry-standard techniques and processing algorithms developed in-house and by OIE research laboratory, including a cloud-index algorithm that produces consistent results when used with the large number of satellites that must be combined to construct a global dataset.

The Vaisala Xweather Solar Model 3 uses the Xweather Solar Model 3 GHI database. It is computed thanks to McClear clear-sky model (i.e. the GHI in clear-sky conditions) and from the cloud opacity extracted from satellite images by Heliosat-V method:



## 2.1 Spatial and temporal coverage

Vaisala Xweather Solar Model 3 database started with satellite images (3 km resolution) of MSG 0° (Meteosat Second Generation) satellites covering Europe, Africa, Middle East and Brazil, available in June 2025. Vaisala extended it to GOES East and West satellites (1 km resolution) covering North and South America at the end of 2025.

Additional satellites (Himawari over East of Asia and Australia, IODC over West of Asia) are planned early 2026 to reach a global coverage.

To prepare Meteosat-10 (Meteosat Second Generation) decommission (planned by EUMETSAT end of 2027), Vaisala Xweather Solar Model 3 database will add Meteosat-12 (Meteosat Third Generation) early 2026.



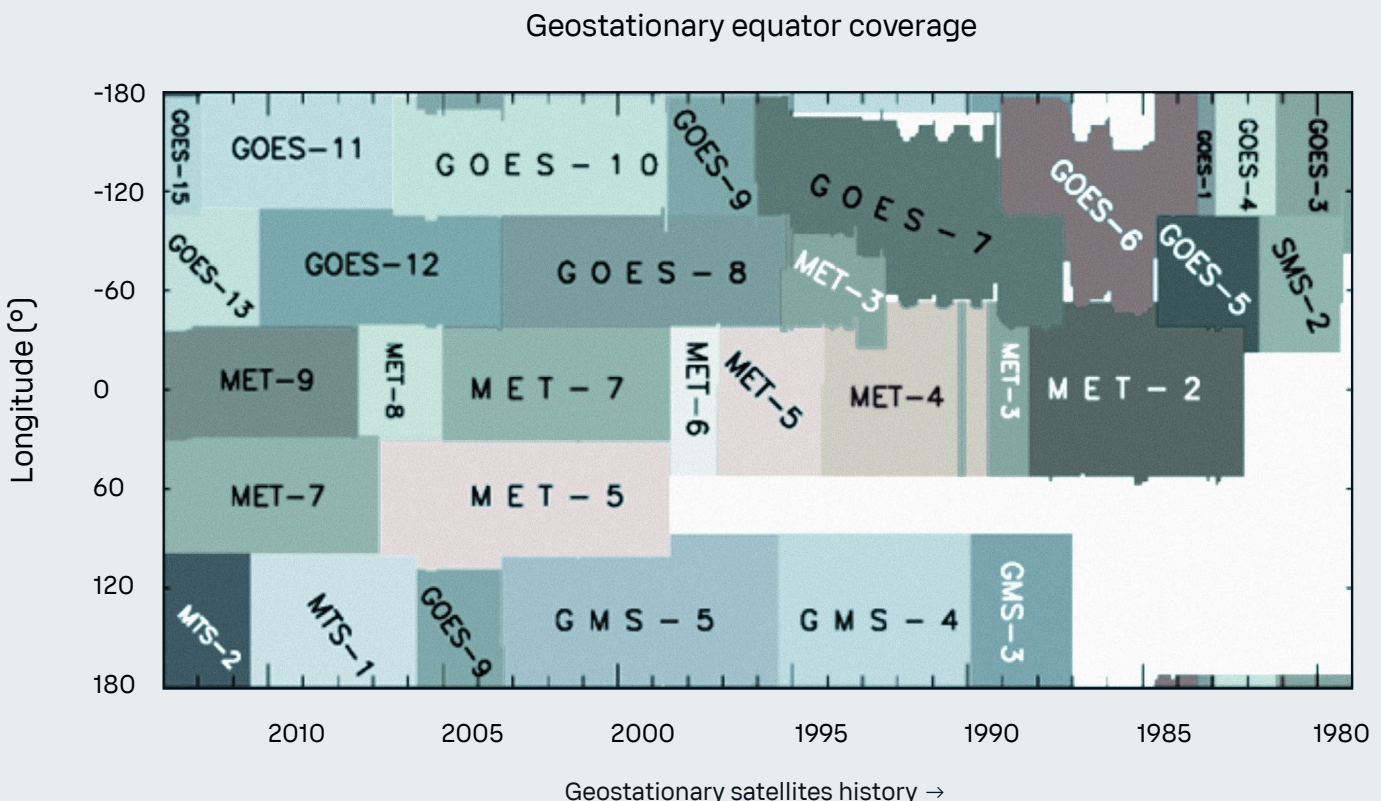
Geostationary satellites

Parameters	Description
Spatial coverage	Land surface and coastal seas between latitudes 66°N to 66°S. Longitudes from 159°E to 66°E end of 2025 (worldwide coverage planned in 2026).
Time representation	Time series since Feb 2004 in Meteosat 0° field of view (Meteosat 8 to 11), since Jan 2004 in GOES East and West fields of view (GOES 8 to 19).
Spatial (grid) resolution	<p>Satellite resolution: 3 to 12 km for Meteosat satellites, depending on the latitude. 1 to 4 km for GOES satellites, depending on the latitude.</p> <p>Enhanced resolution 90m thanks to altitude correction and computation of the relief shadows</p>
Temporal resolution (time step)	<p>Primary satellite time series: 15 minutes for Meteosat satellites, from 15 to 30 minutes for GOES satellites.</p> <p>Derived data products:</p> <ul style="list-style-type: none"> <li>Aggregated into hourly, daily, and monthly values</li> <li>Aggregated into monthly and yearly long-term average values</li> <li>Interpolated solar resource time series: 1-minute and 5-minutes time step</li> </ul>

## 2.2 Key features

Vaisala Xweather Solar Model 3 database estimates downwelling solar irradiance at the Earth surface (aka GHI) using data from a large variety of satellite imagers:

- Worldwide coverage of GHI (planned in 2026)
- Cloud-index method (does not require multiple spectral bands)
- Compatible with several generations of satellites
- Do not require several years of satellite images
- Use independent high-quality albedo
- State-of-the-art performance
- Spatial consistency at satellite frontiers



## 2.3 Description of the Heliosat-V method

Vaisala Xweather Solar Model 3 database is based on Heliosat-V method, which is described in detail in [Tournadre 2020].

Downwelling surface solar irradiance (DSSI) - also called Global Horizontal Irradiation (GHI) - is the solar part of the downwelling irradiance at the surface of the Earth and on a horizontal unit surface. The GHI considers the irradiance coming from all directions of the hemisphere

above the surface: the irradiance coming from the direction of the Sun, usually referred to as beam horizontal irradiance, plus a diffuse component due to scattering caused by the atmosphere (clouds, gases, aerosols) and reflection by the surface, usually referred to as diffuse horizontal irradiance.

The knowledge of GHI variations in space and time is of primary importance for various fields such as the Earth

sciences, solar energy industries, agriculture, or some medical fields. To meet all these needs, ideal information on GHI would feature high spatio-temporal resolution, coverage of the entire Earth surface, and the longest period possible. Long time series of data are notably useful for identifying statistics of long-term inter-annual to multi-decadal variability and possible trends if bias and standard deviation of the error requirements are reached.

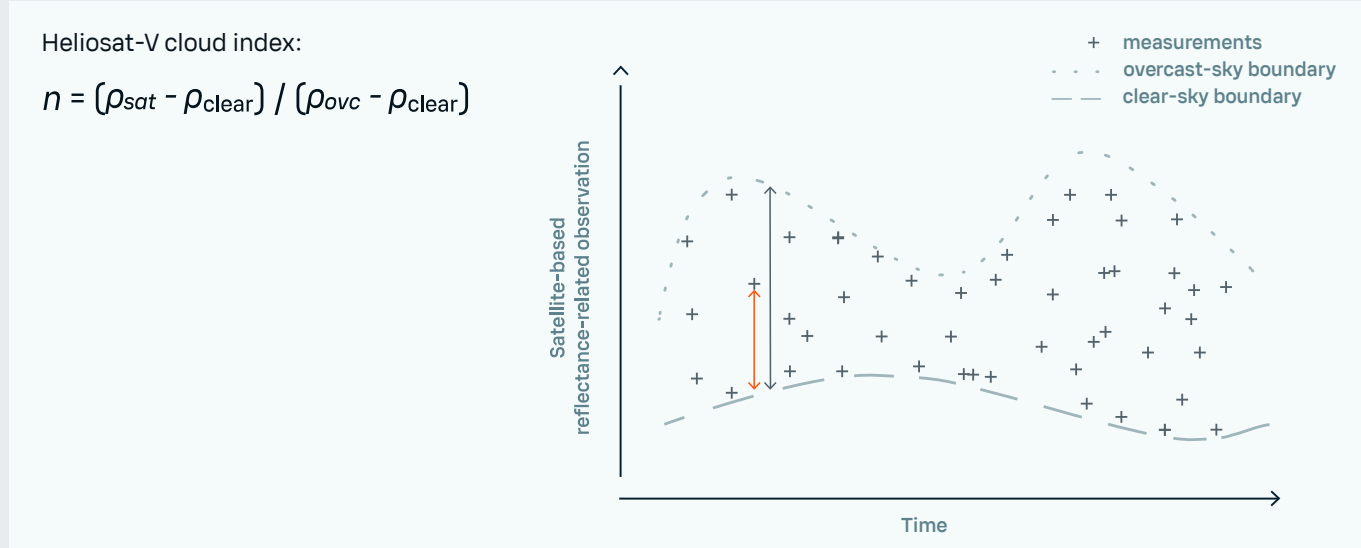
Different approaches already exist to produce such GHI data. Sources of data mainly include ground pyranometric measurements, numerical weather prediction modeling, and satellite-based remote sensing [Sengupta 2021]. Satellite-based methods are an efficient and accurate way to produce kilometric and sub-hourly resolved multidecadal time series of GHI. A more comprehensive review of pros and cons of different methods is notably described in [Huang 2019].

Today, the information from multi-channel satellite measurements offers the possibility of deriving cloud physical properties and then computing cloud attenuation of the solar radiation with methods like FARMS [Xie 2016] and Heliosat-4 [Qu 2017]. Such methods are especially advantageous for highly reflective regions, where clouds are difficult to discriminate from the ground. Nevertheless, they require information on more than one spectral channel, limiting their usage to recent satellites.

Another group of methods, labeled as "cloud-index methods", can produce estimates of downwelling surface solar irradiance from the visible imagery of satellite radiometers without external knowledge on cloud physical and optical properties. This gives them potential to retrieve multi-decadal time series including from the imagery of older satellites.

Heliosat-V is a new way of retrieving the cloud index from a large variety of satellite instruments. To reach its versatility, the method uses simulations from a fast radiative transfer model to estimate overcast (cloudy) and clear-sky (cloud-free) satellite scenes of the Earth's reflectances. Simulations consider the anisotropy of the reflectances caused by both surface and atmosphere and are adapted to the spectral sensitivity of the sensor. The anisotropy of ground reflectances is described by a bidirectional reflectance distribution function model and external satellite-derived data.

The cloud index quantity derives from the radiances measured by satellite sensors and relates them to the extinction of the GHI caused by clouds. The greater the cloud index, the greater the extinction, and the smaller the GHI. More precisely, the cloud index can be used as an empirical proxy for effective cloud transmissivity. The latter, also named "clear-sky index" within the scientific community of solar energy, is defined as the ratio of the all-sky surface irradiance to the clear-sky surface, i.e. the GHI in cloud-free conditions.



The GHI is then computed thanks to McClellan clear-sky model:

$$\text{GHI} = \text{GHI}_{\text{clear\_sky}} \cdot K_{\text{clearness}}$$

with:

$\text{GHI}_{\text{clear\_sky}}$  : GHI under clear sky condition

$K_{\text{clearness}}$  : clearness index

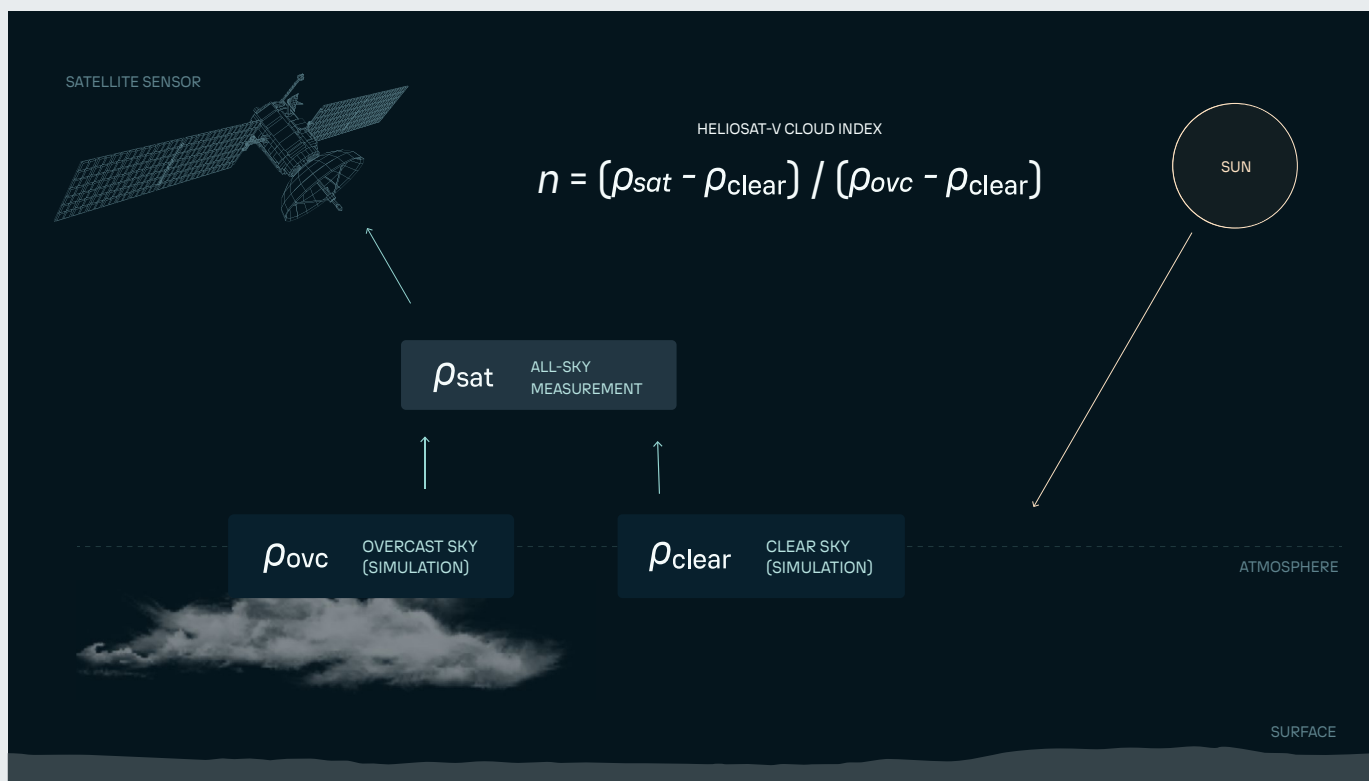
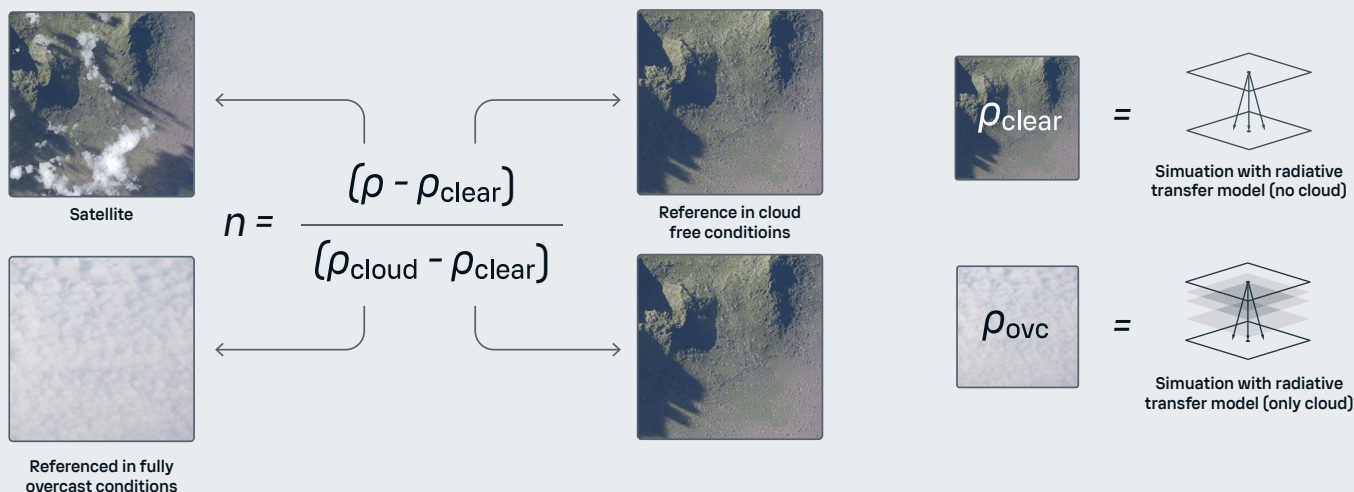
$$K_{\text{clearness}} \approx 1 - n$$

with:

$n$  : cloud index

### 2.3.1 Heliosat-V cloud-index computation

As stated above, Heliosat-V is a method approximating the attenuation of GHI radiation by clouds with a cloud index,  $n$ . Here, the cloud index components are reflectances considered at the top of the atmosphere (TOA).

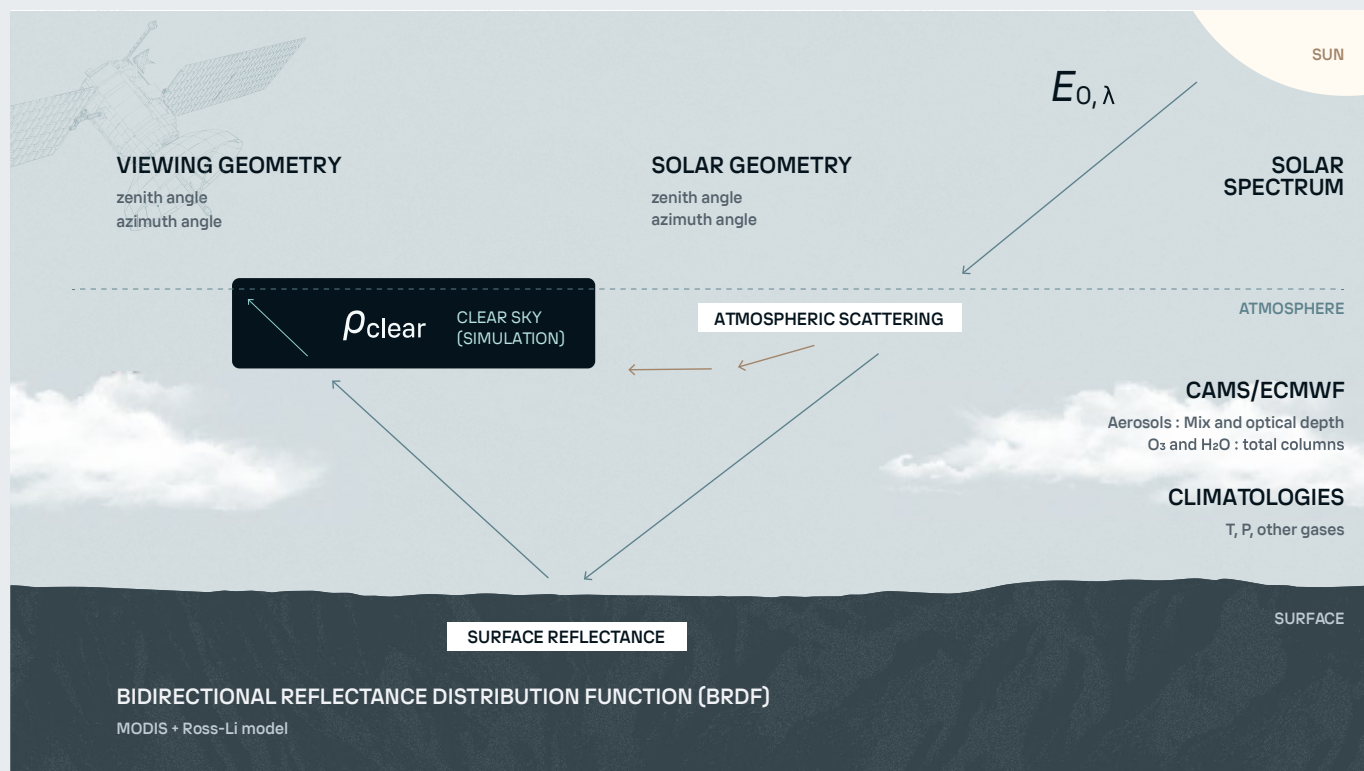


Where  $\rho_{\text{sat}}$  is the reflectance measured by the radiometer for the given spectral channel, while  $\rho_{\text{clear}}$  and  $\rho_{\text{overcast}}$  are estimates of the reflectance that would be measured by the same sensor for, respectively, a clear-sky scene, and an overcast scene, i.e. with an optically thick cloud covering the whole pixel considered.

### 2.3.2 The clear-sky reflectances $\rho_{\text{clear}}$

We use libRadtran radiative transfer model [Emde 2016] to estimate what a spaceborne optical imaging system would measure in clear-sky conditions, for a given radiometric channel. The reflective properties of land surfaces are described with the Ross-Li model

of bidirectional reflectance distribution function and the Moderate Resolution Imaging Spectroradiometer (MODIS) embedded on Terra and Aqua satellites [Wanner 1997].



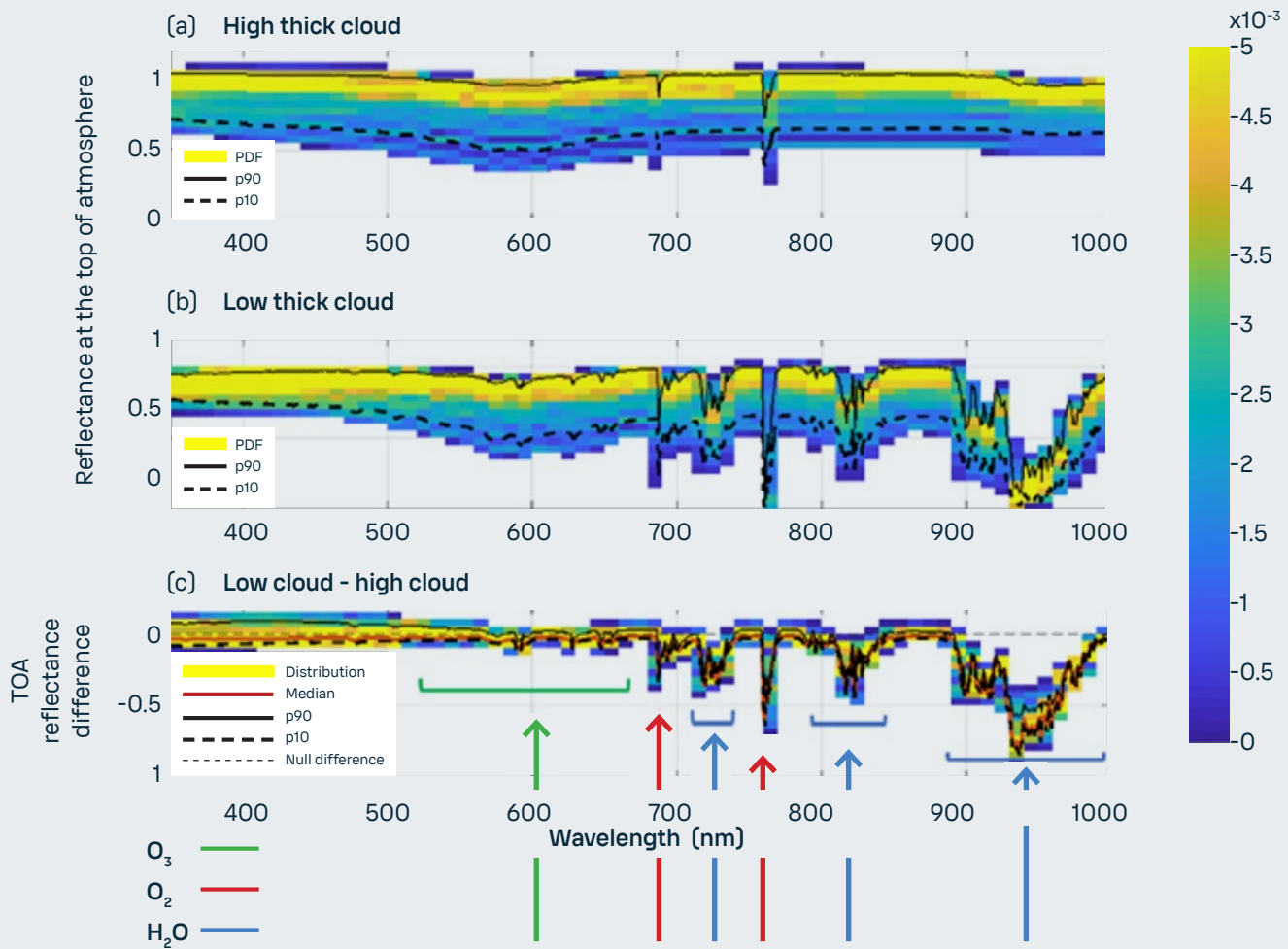
Heliosat-V speeds up the computations using look-up tables (LUT) and Machine Learning models trained from radiative transfer simulations:



### 2.3.3 The overcast-sky reflectances povc

The simulations for a low thick cloud (cloud top height at 500 m) and a high thick cloud (cloud top height at 15 km) show in general a good agreement, except

in absorbing bands of O<sub>2</sub> and H<sub>2</sub>O, and for short wavelengths where scattering becomes increasingly significant:

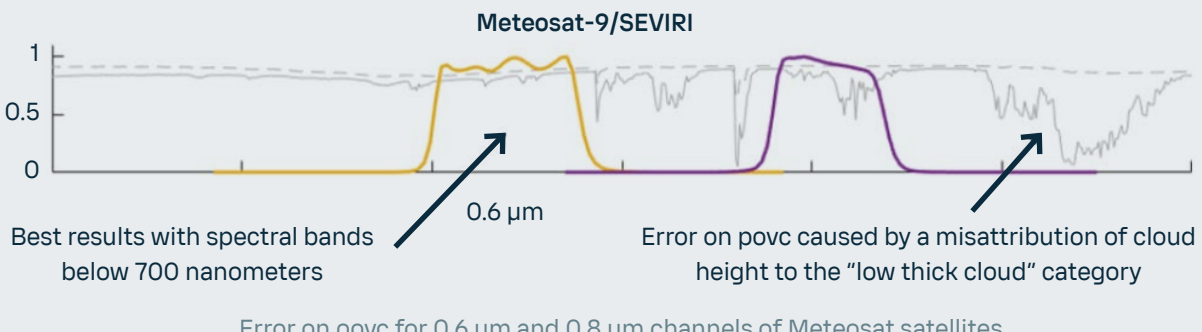


Two upper rows: simulated TOA reflectance in overcast conditions povc with a thick liquid cloud.

Third row: error on povc caused by a misattribution of cloud height to the "low thick cloud" category. Green, red and blue arrows indicate spectral regions with main absorption features from O<sub>3</sub>, O<sub>2</sub> and H<sub>2</sub>O, respectively.

For Meteosat satellites, better results from the channel 0.6  $\mu\text{m}$  could be attributed to a smaller influence of the

cloud top height, compared to the 0.8  $\mu\text{m}$  channel which is affected by water vapor absorption:



An alternative way is therefore to produce look-up tables (LUT) from radiative transfer simulations. As no information is provided on the actual cloud vertical structure, povc is calculated as:  $povc = (povc,high + povc,low) / 2$

where  $povc,high$  and  $povc,low$  are respectively derived from the high and low liquid cloud LUTs, interpolated on the viewing and solar geometries of the satellite time series and adapted to the spectral response function of radiometric channels.

### 2.3.4 McClear clear-sky model

The clear-sky surface irradiance is given by the version 3 of the McClear model [Gschwind 2019]. The McClear model is a fast and accurate model that provides clear-sky estimation of GHI with an absolute bias below 21 W/m<sup>2</sup> and a standard deviation error below 25 W/m<sup>2</sup> for 6 BSRN stations used in this paper.

The McClear model was fed with the partial aerosol optical depths at 550 nm from CAMS reanalysis and CAMS IFS. It is also fed by water vapor atmospheric total columns and the ozone total columns provided by ECMWF.

### 2.3.5 Inputs (cloud-index part)

- **Satellites images:**
  - (MSG-0°, MSG-IODC, Himawari, GOES-W, GOES-E)
- **Atmospheric variables:**
  - AOD: CAMS reanalysis and CAMS IFS (analysis + forecast)
- **Surface properties:**
  - MODIS BRDF (albedo)
- **Angles:**
  - Solar geometry: provided by Solar Geometry 2 library
  - Viewing geometry

### 2.3.6 Inputs (clear-sky part)

- **Weather variables:**
  - AOD: CAMS reanalysis and CAMS IFS (analysis + forecast)
- **Surface properties:**
  - MODIS BRDF (albedo)
  - Altitude (SRTM)
- **Angles:**
  - Solar geometry: provided by Solar Geometry 2 library

### 2.3.7 Sources of errors in GHI computation

Cloud-index methods are sensitive to estimates of clear-sky reflectances at the top of the atmosphere (TOA) *pclear*, to the accuracy of overcast reflectances *povc* and to the contrast between clear-sky and overcast scenes.

For Meteosat satellites, better results from the channel 0.6  $\mu\text{m}$  could be attributed to a smaller influence of the cloud top height, compared to the 0.8  $\mu\text{m}$  channel which is affected by water vapor absorption.

The choice of a spectral linear interpolation between MODIS channels to simulate surface reflectances in SEVIRI channels contributes significantly to biases observed in *pclear* simulations, in particular for the 0.8  $\mu\text{m}$  channel with vegetated surfaces.

The surface reflectivity is lower for shorter wavelengths in general. Selecting a channel for which the surface reflectivity is low will favor a high contrast between clear-sky and overcast scenes and improve the precision in the computation of the cloud index.

Our ability to reproduce reflectances at the top of the atmosphere in overcast conditions depends also on our knowledge of cloud properties, including their scattering phase function, tridimensional structure and top height.

The introduction of radiative transfer simulations in

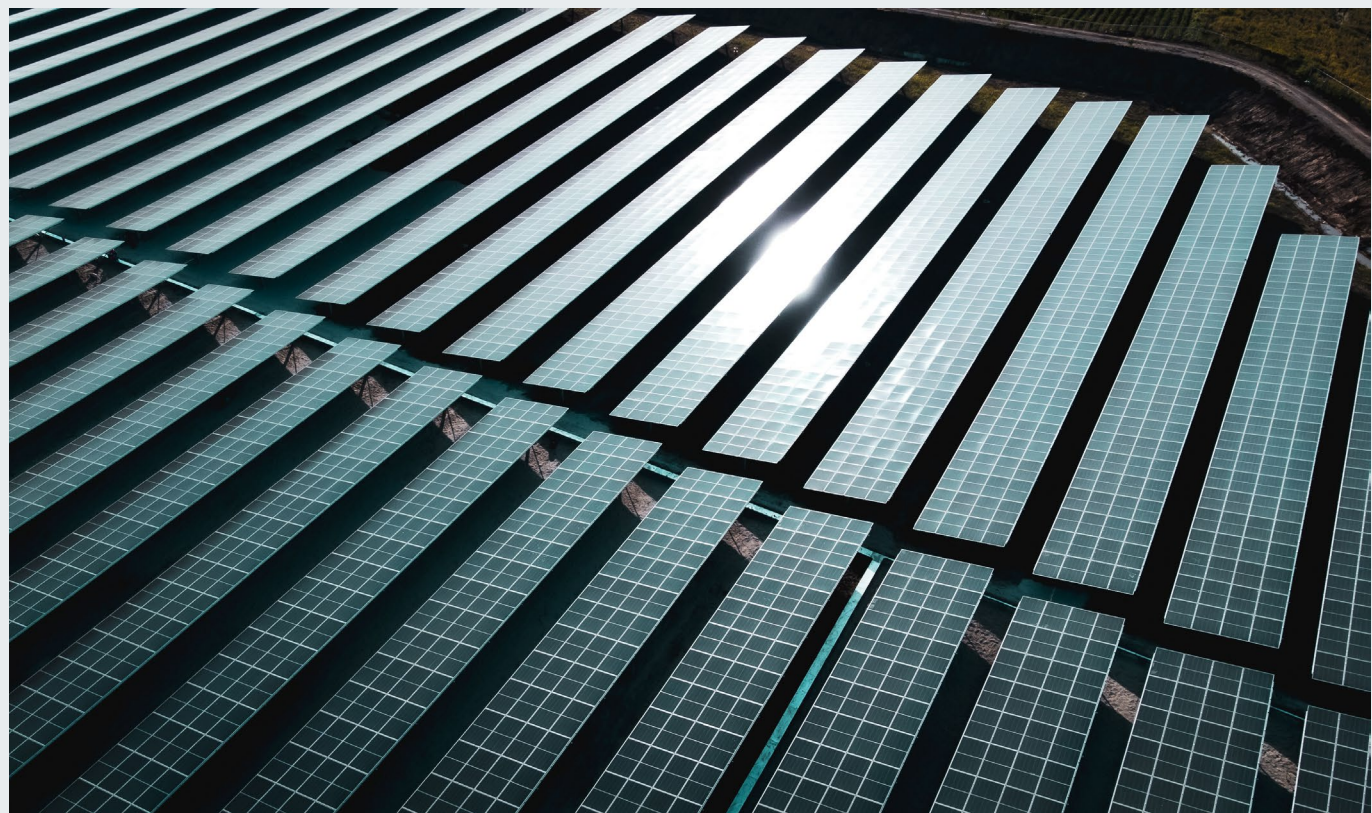
the computation of the cloud index also enhances the importance of an accurate calibration of satellite radiance measurements.

The simple relationship between the cloud index and the clear-sky index used here explains part of the errors in DSSI estimates.

Finally, the quality of the results depends also on the quality of the clear-sky surface irradiance model: the example of the McClear model shows typical biases of 3 % for the studied stations, when compared to BSRN irradiance data.

The knowledge on atmospheric composition in absorbing and scattering species and on surface reflectivity properties is notably lower for past periods like 1980's than for today. Also, the absolute calibration of satellite imagery can be more uncertain, without on-orbit calibrated instruments. Many inputs of the method have very different degrees of quality, depending on the period considered: the composition of the clear-sky atmosphere (aerosols and gases), surface properties, external clear-sky irradiance model.

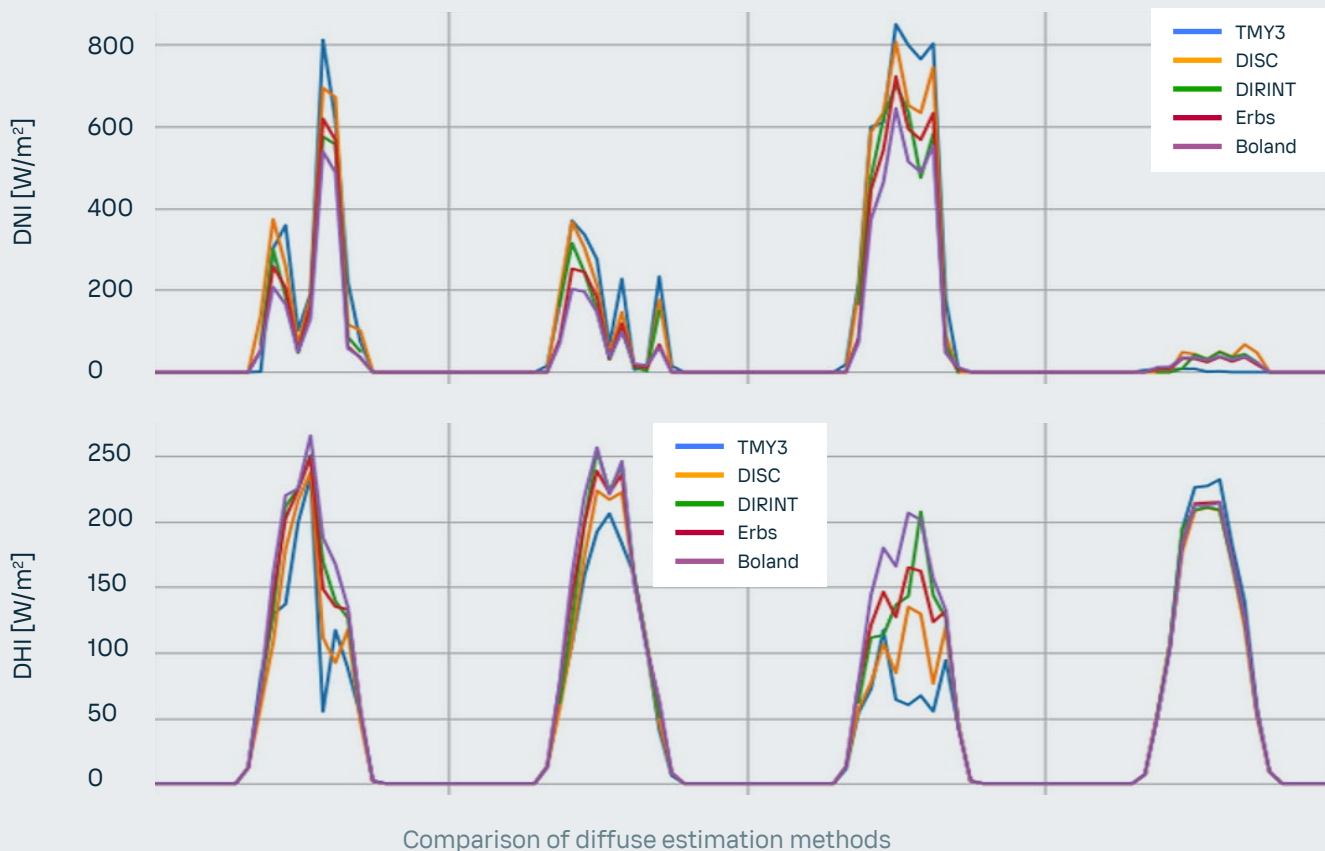
Global coverage of DSSI information obviously requires also to deal with ocean surfaces and snow-covered regions, and this will need to be treated in the future.



## 2.4 Post-processing

From GHI, other solar irradiance components (direct, diffuse and reflected) are calculated. Direct Horizontal Irradiance (DHI) and Direct Normal Irradiance (DNI)

are calculated by the Erbs model [Erbs 1982]. Diffuse horizontal irradiance is derived from GHI and DHI.



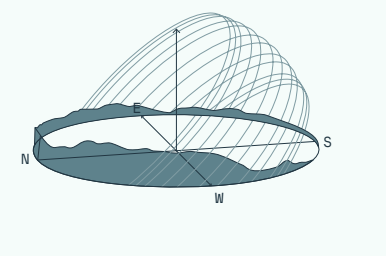
The calculation of Global Tilted Irradiance (GTI) from Global Horizontal Irradiance (GHI) treats direct and diffuse components separately. While estimating the direct component is straightforward, determining diffuse irradiance on a tilted surface is more complex due to limited information on shading and the albedo of surrounding objects. To convert diffuse horizontal irradiance to a tilted surface, Vaisala Xweather Solar Model 3 employs the Perez-Driesse model [Driesse 2024].

**Note:** Xweather Solar Model 3 supports 1D and 2D sun tracking (aka DNI).

The model simulating terrain effects—such as elevation and shading—is based on high-resolution altitude and horizon data. Xweather solar model 3 utilizes the COP90 terrain database for this purpose.



Hill shading in the French Alps



# Validation

3

Solar radiation model accuracy is assessed by comparing model outputs with ground-based measurements. The reliability of this comparison depends on instrument precision, maintenance practices, and the measurement accuracy at each station.

## 3.1 Definition of the indicators

The computed statistics include those most used in the solar industry, such as mean bias error (MBE), mean absolute error (MAE), and hourly root mean square error (RMSE). Mean bias error (MBE) provides information about the average difference in the mean over the entire dataset when compared against observations. Mean absolute error (MAE) measures the average magnitude of the deviation between the ground station and the models. Root mean square error (RMSE) also

measures the average magnitude of the deviation, but uses quadratic weighting, which results in large errors carrying more weight.

A smaller RMSE value means that the dataset more closely tracks observations on an hour-by-hour basis. Together MBE, MAE, and hourly RMSE can be used to assess the accuracy of a solar dataset compared to observations.

## 3.2 Measurements

The Vaisala Xweather Solar Model 3 database is currently generated from Meteosat 0°, GOES East and GOES West satellites imagery. It has been compared to 87 locations where high-quality in situ measurements of GHI are available from the Baseline Surface Radiation Network (BSRN), the EnerMENA Meteorological Network in the MENA Region, the validation dataset of the IEA PVPS, the Energy Sector Management Assistance Program (ESMAP), the SAURAN national program in South Africa and the

Brazilian National Institute for Space Research INPE.

Equipment used to measure GHI have varying uncertainty estimates over an annual basis. The best equipment has uncertainty of less than 1% at a 95% confidence level, but most equipment deployed for solar project measurements is in the 1.5–2% range and some of the second-class equipment deployed is closer to 4–6% uncertainty at the 95% confidence level.

### 3.3 Quality check

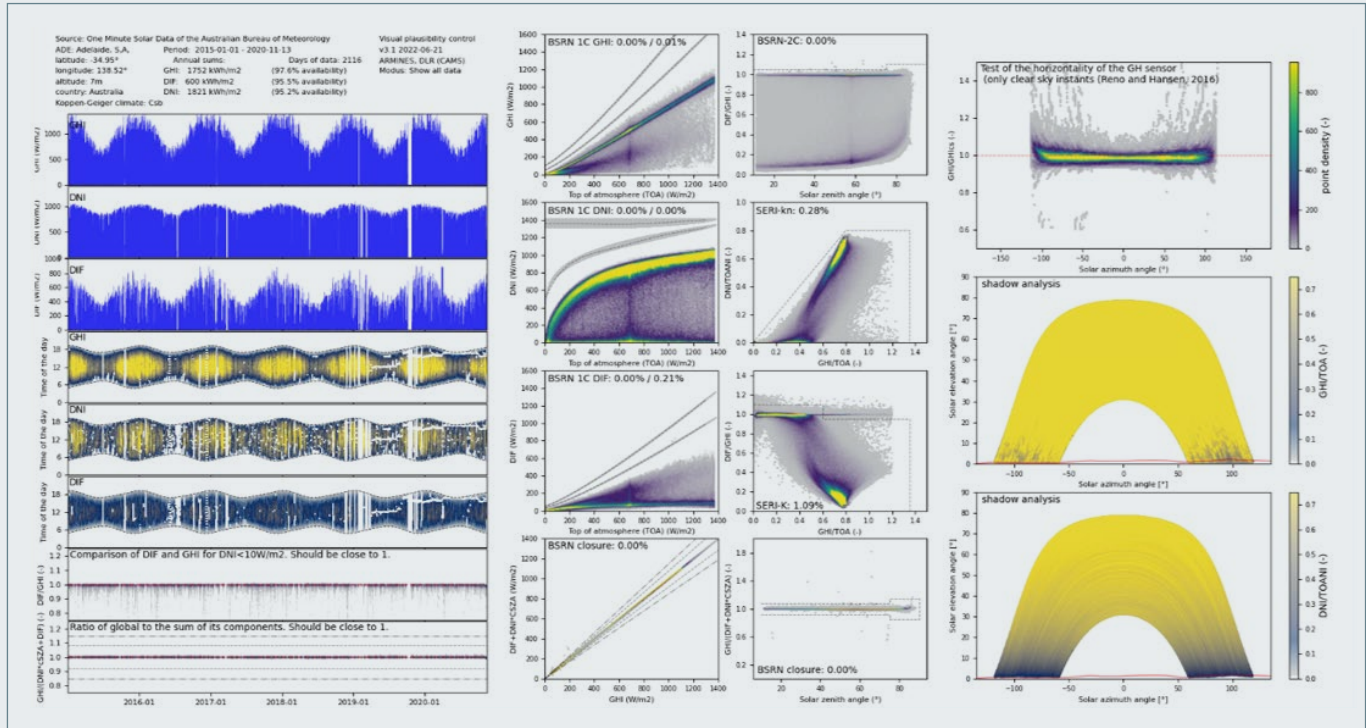
Only quality-controlled measurements from high-quality sensors can be used for objective validation of satellite-based solar model, as issues in the ground-measured data would result in a skewed evaluation.

The data used in the validation of Vaisala Xweather Solar Model 3 comply with the requested features described in the table below. Vaisala did quality control of each

observations station using Libinsitu quality control tool (<https://libinsitu.readthedocs.io>), and anomalous measurements from each station were removed from the results.

Requirements for ground-measured data used in Xweather Solar Model 3 validation:

Requirement	Description	Comments
High accuracy instruments	“Class A” pyranometers	The highest quality and well operated GHI data can have an uncertainty in the range of $\pm 2$ to $\pm 3\%$ .
Long enough period measured	At least 12 months of data	In general, the longer period, the better; one year is the minimum for capturing possible seasonal behavior
Data measured in high temporal resolution	15 minutes values	Sub-hourly values are required for a proper Quality Check
Data filtered using quality control procedures applied	Soiling Condensation Misalignment Miscalibration Shadowing  Other data issues	Both automated and visual checks are used for identifying incorrect values measured by the ground sensors



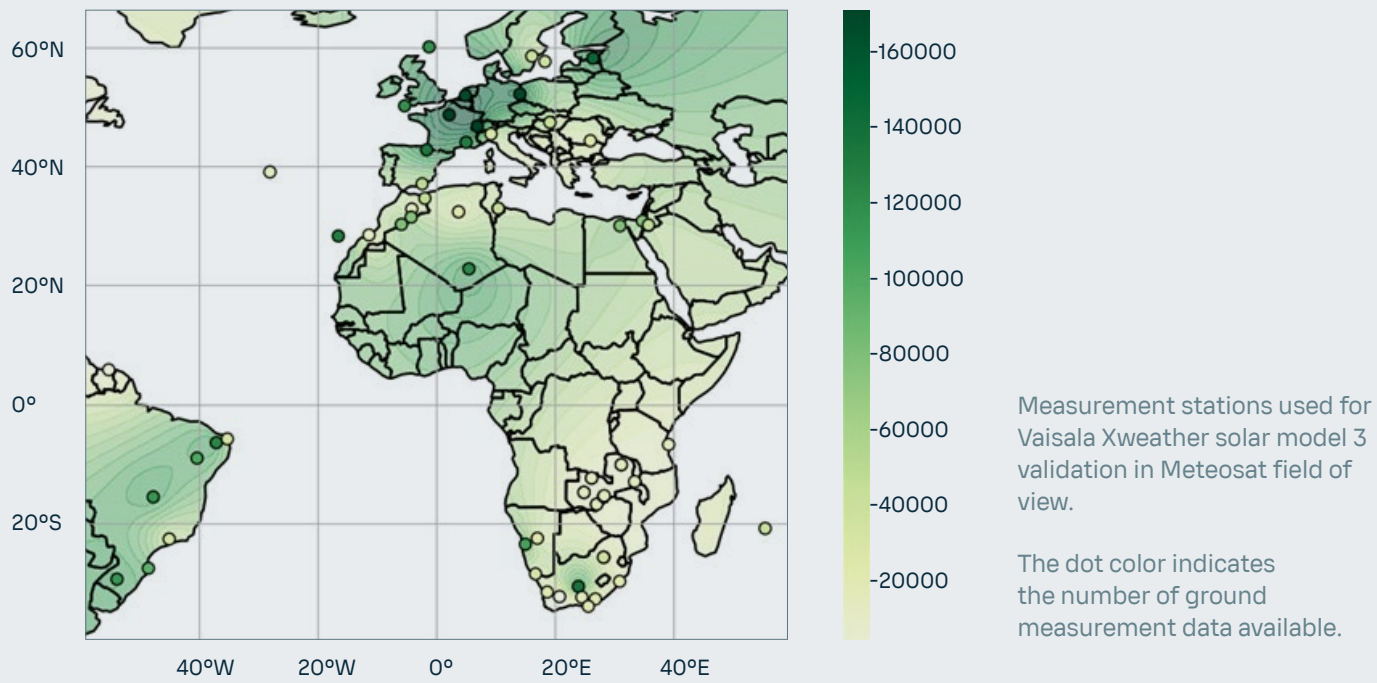
Libinsitu quality control tool

## 3.4 Validation across Meteosat field of view

### 3.4.1 List of measurement stations

Vaisala Xweather solar model 3 validation was performed using observations from 63 high-quality measurement stations across Meteosat 0° satellites field of view. For these satellites, Vaisala used stations from the Baseline Surface Radiation Network (BSRN), the EnerMENA

Meteorological Network in the MENA Region, the validation dataset of the IEA PVPS, the Energy Sector Management Assistance Program (ESMAP), the SAURAN national program in South Africa and the Brazilian National Institute for Space Research INPE.



The measurement stations used by Vaisala for this validation are in the next table (sorted by latitude):

Name	Country	latitude (°)	longitude (°)	altitude (m)	Network
Lerwick	United Kingdom	60.1389	-1.1847	80	bsrn
Norrköping	Sweden	58.582	16.148	53	iea pvps
Toravere	Estonia	58.254	26.462	70	bsrn
Visby	Sweden	57.673	18.345	49	iea pvps
Lindenberg	Germany	52.21	14.122	125	bsrn
Cabauw	The Netherlands	51.968	4.928	0	bsrn
Camborne	United Kingdom	50.2167	-5.3167	88	bsrn
Palaiseau	France	48.713	2.208	156	bsrn
Budapest-Lorinc	Hungary	47.4291	19.1822	139.1	bsrn
Payerne	Switzerland	46.815	6.944	491	bsrn
Milan RSE Site	Italy	45.476179	9.254559	150	iea pvps
Magurele (MARS)	Romania	44.3439	26.0123	110	bsrn
Carpentras	France	44.083	5.059	100	bsrn
Cener	Spain	42.816	-1.601	471	bsrn
Eastern North Atlantic	Azores	39.0911	-28.0292	15.2	bsrn
Plataforma Solar de Almería	Spain	37.0909	-2.3581	500	iea pvps
Oujda	Morocco	34.65	-1.9	618	enermena

Name	Country	latitude (°)	longitude (°)	altitude (m)	Network
Tataouine	Tunisia	32.974	10.485	210	iea pvps
Tataouine	Tunisia	32.92967	10.45177	276	enermena
Missour	Morocco	32.86	-4.107	1043	enermena
Ghardaia	Algeria	32.386	3.78	463	iea pvps
Erfoud	Morocco	31.49099922	-4.217999935	859	enermena
Sede Boqer	Israel	30.8597	34.7794	500	bsrn
Zagora	Morocco	30.27199936	-5.852000237	783	enermena
Ma'an	Jordania	30.172	35.818	1012	iea pvps
Cairo	Egypt	30.036	31.009	86	enermena
Tan-Tan	Morocco	28.498	-11.322	56	enermena
Izana	Tenerife, Spain	28.3093	-16.4993	2372.9	bsrn
Tamanrasset	Algeria	22.7903	5.5292	1385	bsrn
Paramaribo	Surinam	5.806	-55.2146	4	bsrn
Natal	South Africa	-5.8367	-35.2064	58	iea pvps
Caico	Brazil	-6.4669	-37.0847	165	inpe
Dar Es Salaam	Tanzania	-6.78	39.2	122	iea pvps
Petrolina	Brazil	-9.068	-40.319	387	bsrn
Kasama	Zambia	-10.17165	31.22558	1392	esmap
Kasama	Zambia	-10.17165	31.22558	1381	iea pvps
Mutanda	Zambia	-12.423	26.215	1313	esmap
Mutanda	Zambia	-12.423	26.215	1318	iea pvps
Kasungu	Malawi	-13.0153	33.4684	1067	iea pvps
Kaoma	Zambia	-14.839	24.931	1139	esmap
Kaoma	Zambia	-14.839	24.931	1172	iea pvps
Lusaka	Zambia	-15.39463	28.33722	1264	iea pvps
Chilanga	Zambia	-15.5483	28.24817	1221	esmap
Chilanga	Zambia	-15.5483	28.24817	1226	iea pvps
Brasilia	Brazil	-15.601	-47.713	1023	bsrn
Choma	Zambia	-16.83828	27.07046	1265	esmap
Choma	Zambia	-16.83828	27.07046	1284	iea pvps
Reunion Island University	Reunion, France	-20.9014	55.4836	116	bsrn
Namibian University of Science and Technology	South Africa	-22.56500053	17.07500076	1683	sauran
Cachoeira Paulista	Brazil	-22.6896	-45.0062	574	iea pvps
Gobabeb	Namibia	-23.5614	15.042	407	bsrn
CSIR Energy Centre	South Africa	-25.746519	28.278739	1400	sauran
Uni. Pretoria	South Africa	-25.7531	28.2286	1374	iea pvps
Florianopolis	Brazil	-27.6047	-48.5227	11	bsrn
Richtersveld	South Africa	-28.5608	16.7615	134	iea pvps
Sao Martinho da Serra	Brazil	-29.4428	-53.8231	489	bsrn
Uni. of KwaZulu-Natal Westville (Durban)	South Africa	-29.817	30.945	200	iea pvps
De Aar	South Africa	-30.6667	23.993	1287	bsrn
Vanrhynsdorp	South Africa	-31.61747932	18.73834038	130	iea pvps
South African Astronomical Observatory	South Africa	-32.378	20.812	1761	iea pvps
Graaff-Reinet	South Africa	-32.48546982	24.58581924	660	sauran
University of Fort Hare	South Africa	-32.78461075	26.84519958	540	sauran
Nelson Mandela University	South Africa	-34.0086	25.6653	24	iea pvps

### 3.4.2 Global statistics

The statistics presented in the following sections were computed using only daytime irradiance values, which provide a better indication of the accuracy and value of the dataset for use in resource estimation.

Comparison statistics were calculated for GHI based on the overall MBE, MAE and RMSE at each location, then globally in the satellite field of view.

In average, Vaisala Xweather solar model 3 GHI values show a mean bias error (MBE) of 0.86%, an hourly mean absolute error (MAE) of 9.84%, a root mean square error (RMSE) of 15.06% and a bias standard deviation of 2.72% across Meteosat field of view.

The statistics per station are available in the annex 5.1.

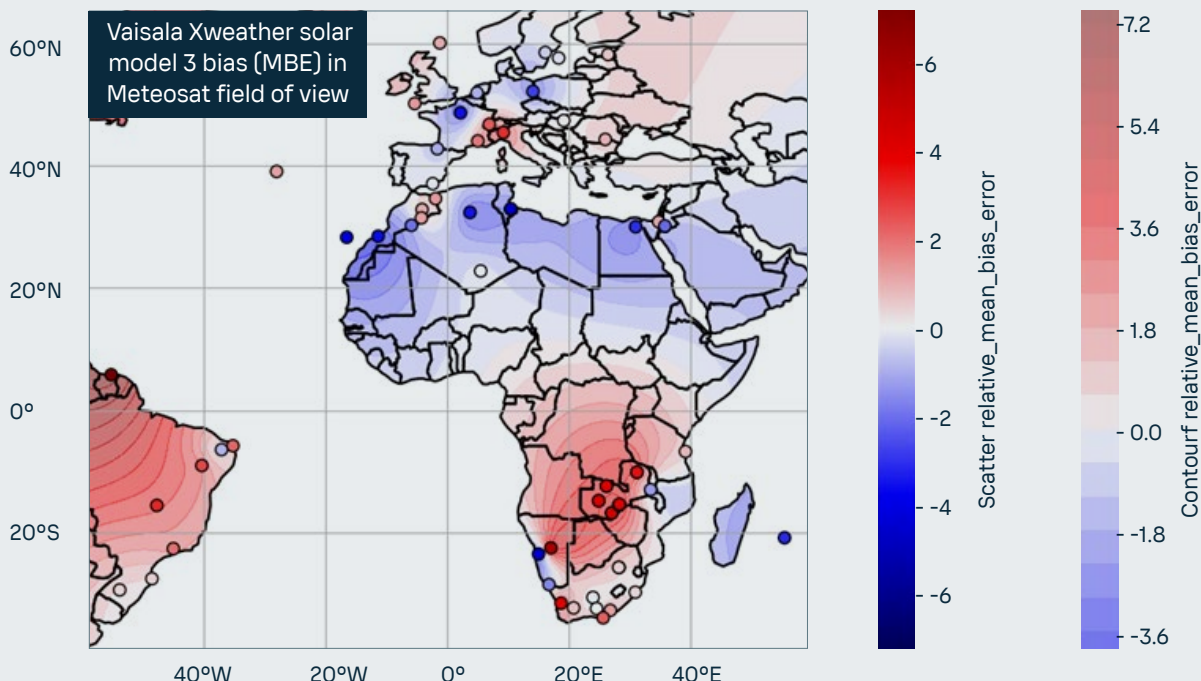
#### 3.4.2.1 Bias

The overall bias results on 63 high-quality stations are:

- Despite the uneven distribution of validation sites, Vaisala Xweather solar model 3 shows stable and consistent performance across all climate zones.
- The overall average bias is low (0.86%). Across all stations, the MBE ranges from -3.62% to 4.95% with 90% confidence. Bias is near zero in Europe, negative in North Africa and the Middle East, and positive in tropical regions.
- Some validation sites are outliers, skewing maximum errors. These include high-altitude stations (e.g. Izaña on top of a volcano) and locations

near the satellite's field-of-view edge, where extreme sun-satellite angles and pixel distortion affect cloud property estimates.

- Key factors influencing model accuracy vary by climate zone. Performance is strong in temperate zones. In tropical areas, persistent broken cloud cover challenges the model's ability to derive optical properties from satellite data. In arid regions, aerosol representation is the main driver of accuracy.
- The model appears to perform well in the sub-Saharan region, though this requires further study due to limited high-quality ground measurements.

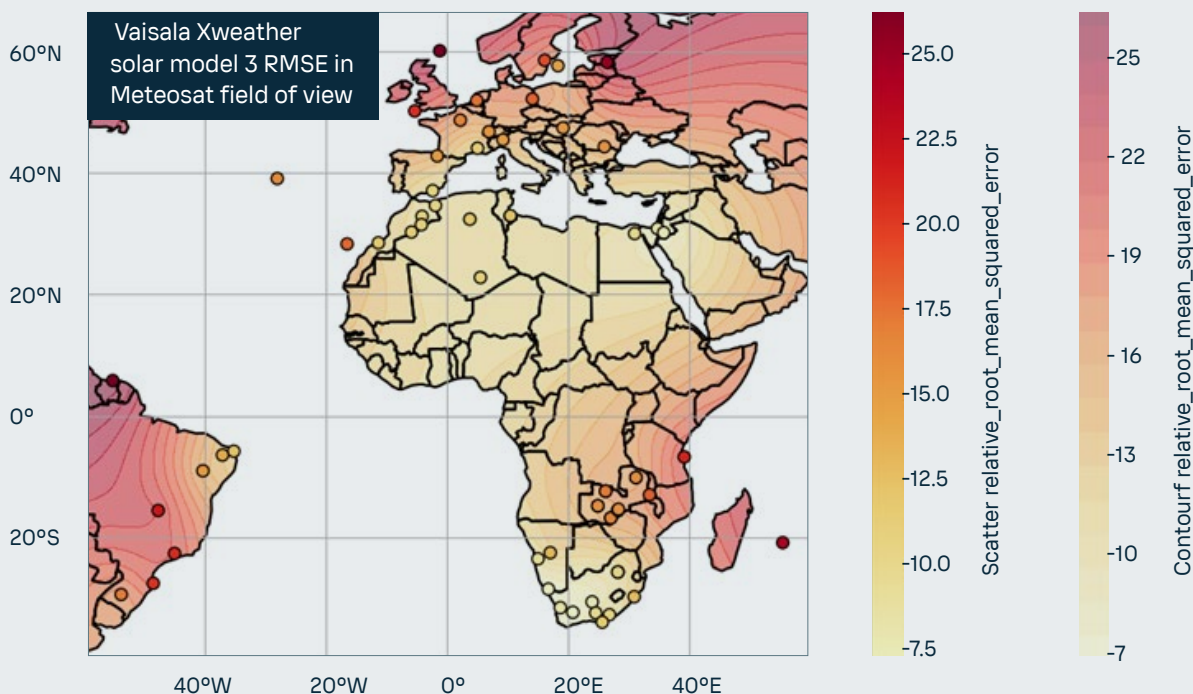


### 3.4.2.2 RMSE

The Root Mean Square Error (RMSE) indicates consistent model performance, with error decreasing as data is aggregated. Specifically, RMSE is higher for hourly data than for daily data, and higher for daily than for monthly values. This trend is expected in satellite-based models due to the nature of the data: satellite imagery has a spatial resolution of several square kilometers, while ground instruments like pyranometers and pyrheliometers measure radiation at a single point.

The overall RMSE results on 63 high-quality stations are:

- The overall hourly RMSE is low (15.06%).
- Xweather Solar Model 3 shows stable and consistent performance across all climate zones.
- The RMSE per station is largely correlated to the distance from the satellite nadir: the RMSE is minimum in the Gulf of Guinea and maximum close to the edge of Meteosat field of view. Like for the bias, locations near the satellite's field-of-view edge suffer from extreme sun-satellite angles and pixel distortion.

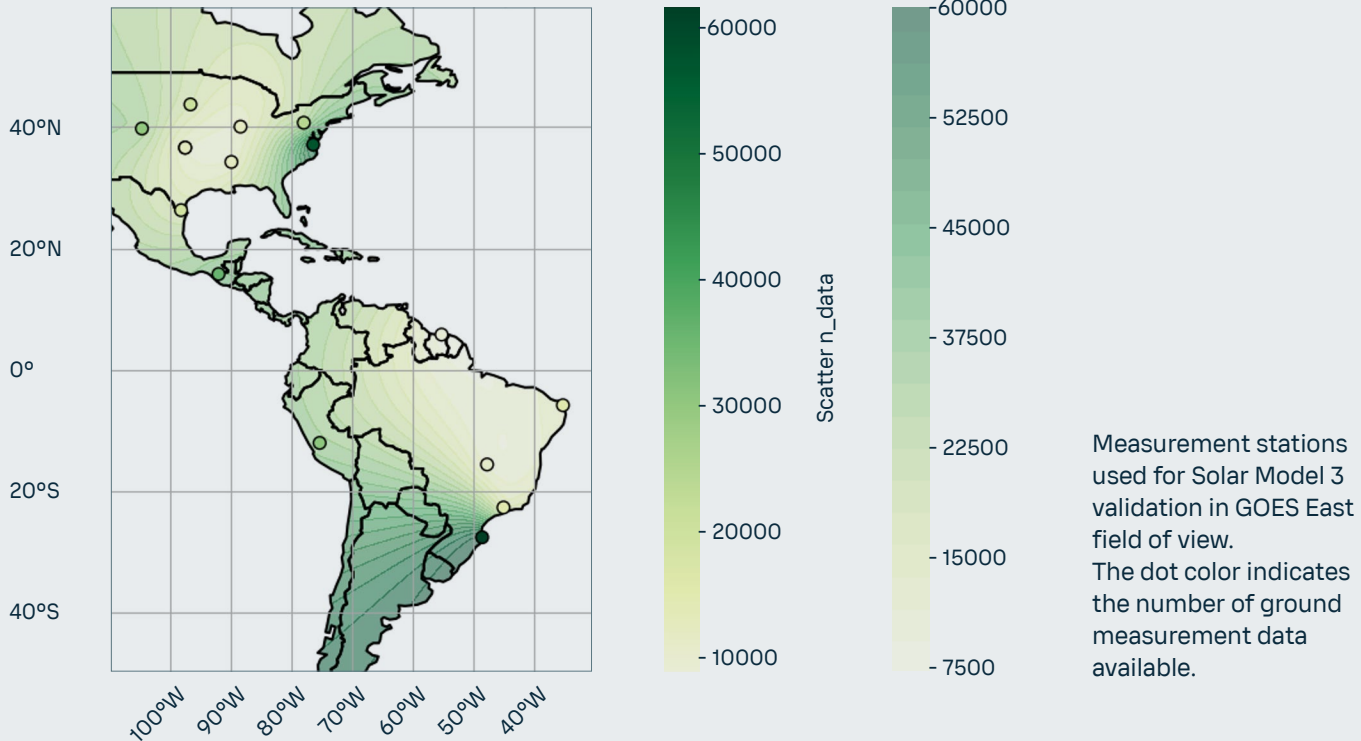


## 3.5 Validation across GOES East field of

### 3.5.1 List of measurement stations

Vaisala Xweather solar model 3 validation was performed using observations from 16 high-quality measurement stations across GOES 16 (GOES East) satellite field of view.

For this satellite, Vaisala used stations from the Baseline Surface Radiation Network (BSRN) and the validation dataset of the IEA PVPS.



The measurement stations used by Vaisala for this validation are in the next table (sorted by latitude):

Name	Country	latitude (°)	longitude (°)	altitude (m)	Network
Sioux Falls	USA	43.73	-96.62	473	bsrn
Rock Springs	USA	40.72	-77.9333	376	bsrn
Bondville	USA	40.0667	-88.3667	213	bsrn
Solar Technology Acceleration Center (So-	USA	39.7569	-104.6203	1674	iea pvps
Langley Research Center	USA	37.1038	-76.3872	3	bsrn
Billings	USA	36.605	-97.516	317	bsrn
Southern Great Plains	USA	36.605	-97.485	318	bsrn
Goodwin Creek	USA	34.2547	-89.8729	98	bsrn
University of Texas Panamerican Solar Radia-	USA	26.3059	-98.1716	45.4	iea pvps
Selegua	Mexico	15.784	-91.9902	602	bsrn
Paramaribo	Surinam	5.806	-55.2146	4	bsrn
Natal	Brazil	-5.8367	-35.2064	58	iea pvps
Observatory of Huancayo	Peru	-12.05	-75.32	3314	bsrn
Brasilia	Brazil	-15.601	-47.713	1023	bsrn
Cachoeira Paulista	Brazil	-22.6896	-45.0062	574	iea pvps
Florianopolis	Brazil	-27.6047	-48.5227	11	bsrn

### 3.5.2 Global statistics

The statistics presented in the following sections were computed using only daytime irradiance values, which provide a better indication of the accuracy and value of the dataset for use in resource estimation.

Comparison statistics were calculated for GHI based on the overall MBE, MAE and RMSE at each location, then globally in the satellite field of view.

In average, Vaisala Xweather solar model 3 GHI values show a mean bias error (MBE) of 1.18%, an hourly mean absolute error (MAE) of 11.11%, a root mean square error (RMSE) of 17.48% and a bias standard deviation of 1.34% across GOES 16 (GOES East) field of view.

The statistics per station are available in the annex 5.1.

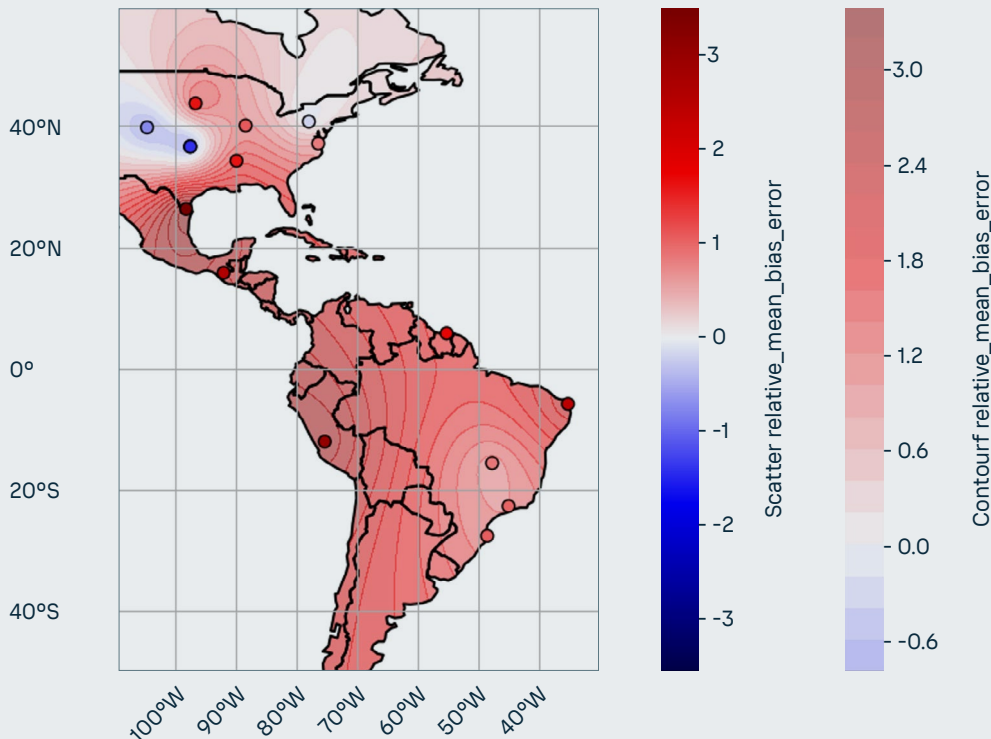
#### 3.5.2.1 Bias

The overall bias results on 16 high-quality stations are:

- Despite the uneven distribution of validation sites, Vaisala Xweather solar model 3 shows stable and consistent performance across all climate zones.
- The overall average bias is low (1.18%). Across all stations, the MBE ranges from -0.9% to 3.14% with 90% confidence. Bias is near zero or slightly negative in North America, and positive in Central and South America.

- Some validation sites are outliers, skewing maximum errors. These include typically high-altitude stations (e.g. Huancayo in Peru) and locations near the satellite's field-of-view edge (no example in this set of stations).
- Key factors influencing model accuracy vary by climate zone. Performance is strong in temperate zones. In tropical areas, persistent broken cloud cover challenges the model's ability to derive optical properties from satellite data. In arid regions, aerosol representation is the main driver of accuracy.

Vaisala Xweather solar model 3 bias (MBE) in GOES 16 (GOES East) field of view



### 3.5.2.2 RMSE

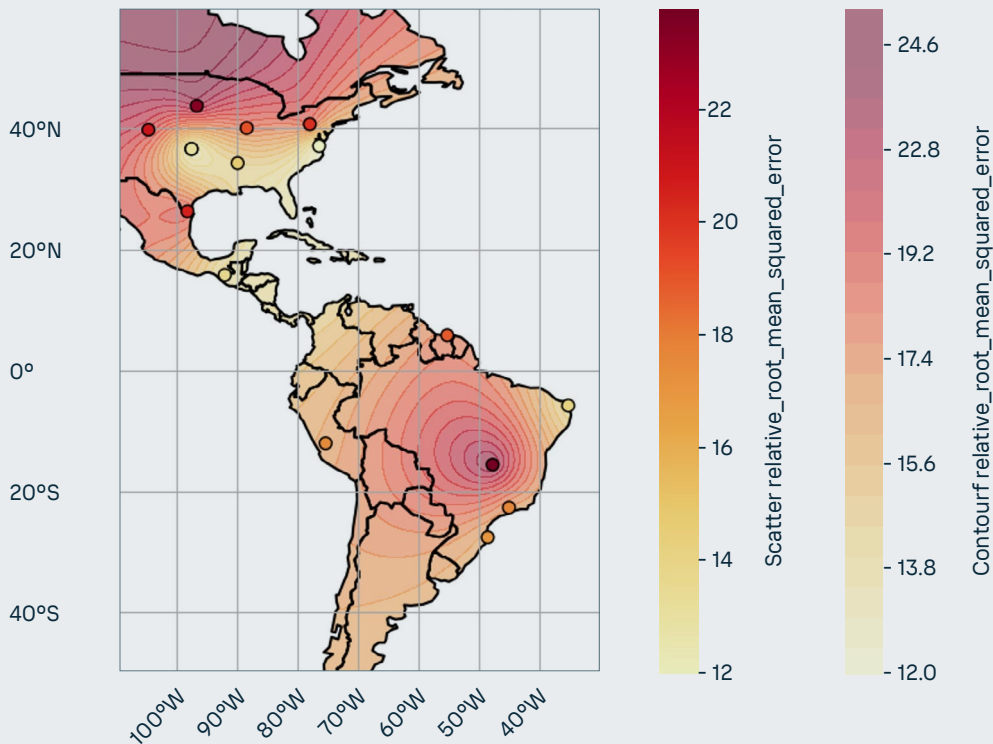
The Root Mean Square Error (RMSE) indicates consistent model performance, with error decreasing as data is aggregated. Specifically, RMSE is higher for hourly data than for daily data, and higher for daily than for monthly values. This trend is expected in satellite-based models due to the nature of the data: satellite imagery has a spatial resolution of several square kilometers, while ground instruments like pyranometers and pyrheliometers measure radiation at a single point.

The overall RMSE results on 16 high-quality stations are:

- The overall hourly RMSE is low (17.48%).
- Vaisala Xweather solar model 3 shows stable and consistent performance across all climate zones.

- Key factors influencing model accuracy vary by climate zone. Performance is strong in temperate zones. In tropical areas, persistent broken cloud cover challenges the model's ability to derive optical properties from satellite data. In arid regions, aerosol representation is the main driver of accuracy.
- The RMSE per station is in general larger for locations near the satellite's field-of-view edge, where extreme sun-satellite angles and pixel distortion affect cloud property estimates. This is visible here at Sioux-Falls and in Canada.

Vaisala Xweather solar model 3 RMSE in GOES 16 (GOES East) field of view

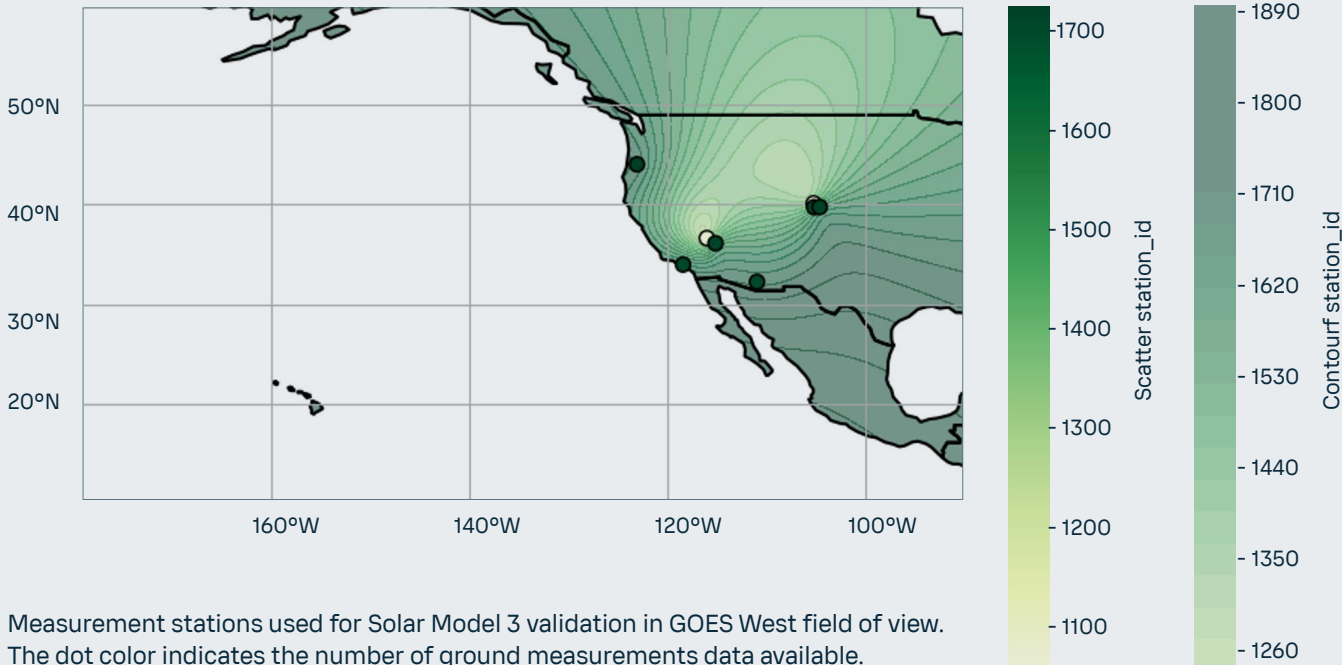


# 3.6 Validation across GOES West field of view

## 3.6.1 List of measurement stations

Vaisala Xweather solar model 3 validation was performed using observations from 8 high-quality measurement stations across GOES 15 (GOES West) satellite field of view.

For this satellite, Vaisala used stations from the Baseline Surface Radiation Network (BSRN) and the validation dataset of the IEA PVPS.



The measurement stations used by Vaisala for this validation are in the next table (sorted by latitude):

Name	Country	latitude (°)	longitude (°)	altitude (m)	Network
University of Oregon (SRML)	USA	44.0467	-123.0743	133.8	iea pvps
Boulder	USA	40.125	-105.237	1689	bsrn
Solar Technology Acceleration Center (SolarTAC)	USA	39.7569	-104.6203	1674	iea pvps
Golden	USA	39.742	-105.18	1829	iea pvps
Desert Rock	USA	36.626	-116.018	1007	bsrn
University of Nevada - Las Vegas	USA	36.107	-115.1425	615	iea pvps
SOLRMAP Loyola Marymount University (RSR)	USA	33.9667	-118.4226	27	iea pvps
SOLRMAP University of Arizona (OASIS)	USA	32.2297	-110.9553	786	iea pvps

### 3.6.2 Global statistics

The statistics presented in the following sections were computed using only daytime irradiance values, which provide a better indication of the accuracy and value of the dataset for use in resource estimation.

Comparison statistics were calculated for GHI based on the overall MBE, MAE and RMSE at each location, then globally in the satellite field of view.

In average, Vaisala Xweather solar model 3 GHI values show a mean bias error (MBE) of 0.36%, an hourly mean absolute error (MAE) of 8.32%, a root mean square error (RMSE) of 13.39% and a bias standard deviation of 2.21% across GOES 15 (GOES West) field of view.

The statistics per station are available in the annex 5.1.

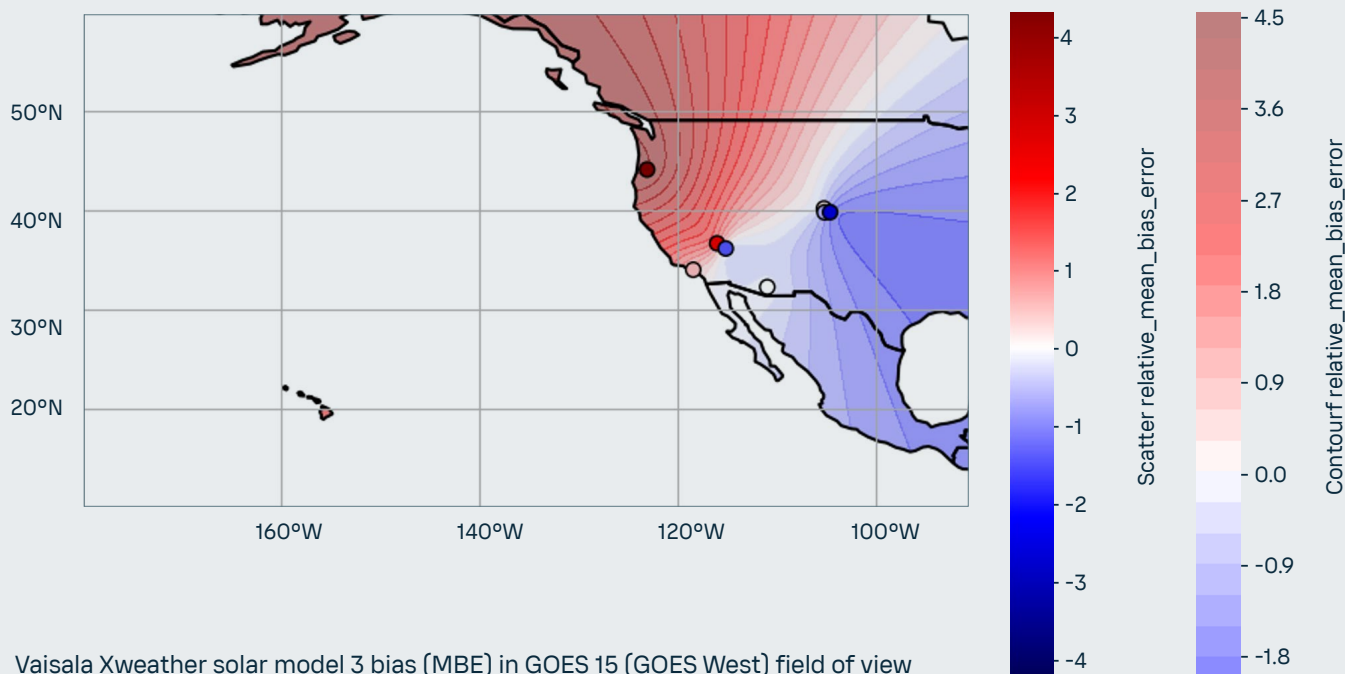
#### 3.6.2.1 Bias

The overall bias results on 8 high-quality stations are:

- Despite the uneven distribution of validation sites, Vaisala Xweather solar model 3 shows stable and consistent performance across all climate zones.
- The overall average bias is low (0.36%). Across all stations, the MBE ranges from -2.22% to 3.71% with 90% confidence. Bias is near zero or slightly negative in the south of the USA and Mexico, and positive in the north of the USA and Canada.
- Some validation sites are outliers, skewing maximum errors. These include typically high-altitude stations (Boulder, SolarTAC and Golden) and

locations near the satellite's field-of-view edge (no example in this set of stations).

- Key factors influencing model accuracy vary by climate zone. Performance is strong in temperate zones. In tropical areas, persistent broken cloud cover challenges the model's ability to derive optical properties from satellite data (not applicable for GOES West). In arid regions, aerosol representation is the main driver of accuracy: it is good in North America.
- The model requires further study in Canada due to the lack of high-quality ground measurements.



### 3.6.2.2 RMSE

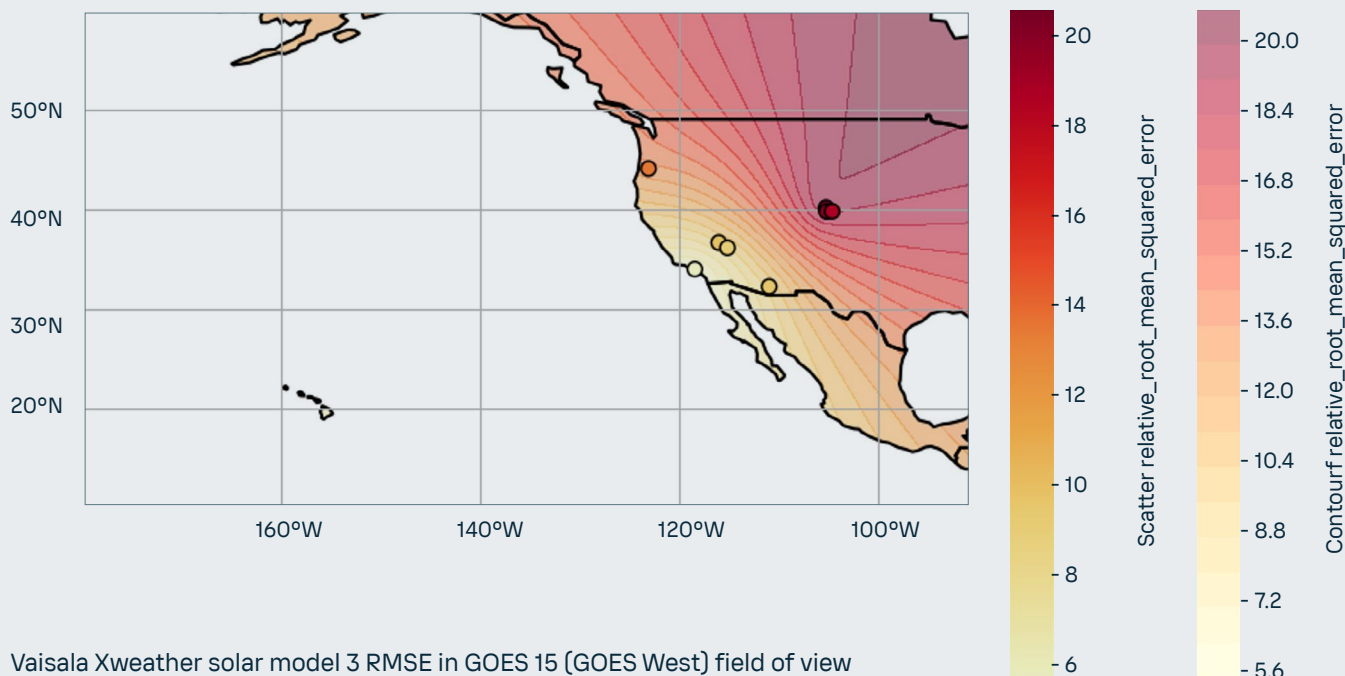
The Root Mean Square Error (RMSE) indicates consistent model performance, with error decreasing as data is aggregated. Specifically, RMSE is higher for hourly data than for daily data, and higher for daily than for monthly values. This trend is expected in satellite-based models due to the nature of the data: satellite imagery has a spatial resolution of several square kilometers, while ground instruments like pyranometers and pyrheliometers measure radiation at a single point.

The overall RMSE results on 8 high-quality stations are:

- Vaisala Xweather solar model 3 shows stable and consistent performance across all climate zones.
- The overall hourly RMSE is low (13.39%). RMSE is low in the south of the USA and Mexico, and larger in the north of the USA and Canada.
- Key factors influencing model accuracy vary by

climate zone. Performance is strong in temperate zones. In tropical areas, persistent broken cloud cover challenges the model's ability to derive optical properties from satellite data (not applicable for GOES West). In arid regions, aerosol representation is the main driver of accuracy: it is good in North America.

- Some validation sites are outliers, skewing maximum errors. These include high-altitude stations (Boulder, SolarTAC and Golden).
- The RMSE per station is in general larger for locations near the satellite's field-of-view edge, where extreme sun-satellite angles and pixel distortion affect cloud property estimates. This is visible in the map below in Canada.
- The model requires further study in Canada due to the lack of high-quality ground measurements.



## 3.7 Comparison with other solar databases

Each provider of satellite-based irradiation performs a validation of its model. The following table shows a comparison of the validation results of Vaisala's models (Vaisala Xweather solar model 3, Helioclim-3, Vaisala 2.1 and CAMS Radiation Service).

Please be aware that this table is only indicative, as the

set of measurement stations selected for Vaisala 2.1 has a worldwide coverage, when Vaisala Xweather solar model 3 is available for Meteosat, GOES East and GOES West, and Helioclim-3 and CAMS Radiation Service are limited to Meteosat field of view. The table will be updated when Vaisala Xweather solar model 3 supports global view, expected Q1 2026.

Model	Solar Model 3 (Meteosat)	Solar Model 3 (GOES East)	Solar Model 3 (GOES West)	Helioclim-3 (Meteosat)	CAMS Radiation Service (Meteosat)	Vaisala 2.1 (Worldwide)
Number of sites	63	16	8	63	63	196
Mean Bias	0.86%	1.18%	0.36%	1.38%	2.31%	1.20%
Bias standard deviation	2.72%	1.34%	2.21%	3.97%	3.87%	4.09%
Mean hourly RMSE	15.06%	17.48%	13.39%	17.05%	16.82%	19.94%

Comparative table with Vaisala Xweather solar model 3, Helioclim-3, CAMS Radiation Service, and Vaisala 2.1

### Sources:

Vaisala 2.1: Vaisala's 2019 validation "Vaisala Global Solar Dataset 2019 Release / Methodology and Validation"  
<https://cdn.energy.vaisala.com/media/papers/solar/Vaisala-SolarValidation-Oct2019-rev1-May2020.pdf>

# Conclusion and perspectives

4

Solar energy production is directly correlated to the amount of radiation received at a project location.

Like all weather-driven renewable resources, solar radiation can vary rapidly over time and space, and understanding this variability is crucial in determining the financial viability of a solar energy project.

Different approaches exist to produce solar data. Sources of data mainly include ground pyranometric measurements, numerical weather prediction modeling, and satellite-based remote sensing.

Heliosat-V method is a new way of retrieving the GHI from a large variety of satellite instruments sensitive. To reach its versatility, the method uses simulations from a fast radiative transfer model to estimate overcast (cloudy) and clear-sky (cloud-free) satellite scenes of the Earth's reflectances. Simulations consider the anisotropy of the reflectances caused by both surface and atmosphere and are adapted to the spectral sensitivity of the sensor.

The cloud index is built to deal with a single radiometric channel in the spectral range 400-1000 nm. It also does not need archives of data to quantify the cloud effective transmissivity. This approach has advantages. First, the concept of the Heliosat-V cloud index enables the use of imagery from geostationary and non-geostationary platforms, an asset to reach an extended spatial coverage. Moreover, the approach has the potential to deal with long time series of imagery from radiometers characterized by different spectral sensitivities and viewing geometries.

Validation results using SEVIRI imagery show that DSSI can be estimated by a cloud index method that does not rely on archives of imagery, with a quality similar to operational satellite-based data products, in terms of RMSE and correlation.

The Vaisala Xweather solar model 3 database is currently generated from Meteosat 0°, GOES East and GOES West satellites imagery. It has been compared to 87 locations where high-quality in situ measurements of GHI are available from the Baseline Surface Radiation Network (BSRN), the EnerMENA Meteorological Network in the MENA Region, the validation dataset of the IEA PVPS, the Energy Sector Management Assistance Program (ESMAP), the SAURAN national program in South Africa and the Brazilian National Institute for Space Research INPE.

In average, results from the Vaisala Xweather solar model 3 and ground-based measurements show a mean bias error (MBE) of 0.36% to 0.86% (depending on the satellite), a bias standard deviation of 1.34% to 2.72%, an hourly mean absolute error (MAE) of 8.32 to 11.11% and an hourly root mean square error (RMSE) of 13.39 to 17.48%.

To clarify the potential of the method for long time series of imagery, we will need to explore how sensitive to the quality of input data the results are. The knowledge on atmospheric composition in absorbing and scattering species and on surface reflectivity properties is notably lower for past periods like 1980's than for today. Also, the absolute calibration of satellite imagery can be more uncertain, without on-orbit calibrated instruments. Many inputs of the method have very different degrees of quality, depending on the period considered: the composition of the clear-sky atmosphere (aerosols and gases), surface properties, external clear-sky irradiance model.

Global coverage of DSSI information obviously requires also to deal with ocean surfaces and snow-covered regions, and this will need to be treated in the future.

# Annex



# 5.1 Statistics per station

## 5.1.1 Meteosat

The statistics of Vaisala Xweather solar model 3 GHI at hourly time step compared to high quality measurements in the field of view of Meteosat 0° satellites are given in the next table:

Name	Country	latitude (°)	longitude (°)	altitude (m)	Network	Mean Bias Error MBE (%)	Mean Absolute Error MAE (%)	Root Mean Square Error RMSE (%)
Lerwick	United Kingdom	60.1389	-1.1847	80	bsrn	1.12	18.17	26.55
Norrköping	Sweden	58.582	16.148	53	iea pvps	-0.59	12.51	19.31
Toravere	Estonia	58.254	26.462	70	bsrn	0.70	15.51	25.38
Visby	Sweden	57.673	18.345	49	iea pvps	-0.25	9.41	14.98
Lindenberg	Germany	52.21	14.122	125	bsrn	-2.80	11.89	18.29
Cabauw	The Netherlands	51.968	4.928	0	bsrn	-0.98	11.82	17.74
Camborne	United Kingdom	50.2167	-5.3167	88	bsrn	1.33	13.58	20.89
Palaiseau	France	48.713	2.208	156	bsrn	-3.55	11.01	16.97
Budapest-Lorinc	Hungary	47.4291	19.1822	139.1	bsrn	0.21	9.91	15.50
Payerne	Switzerland	46.815	6.944	491	bsrn	2.38	10.40	15.80
Milan RSE Site	Italy	45.476179	9.254559	150	iea pvps	3.10	9.87	15.34
Magurele (MARS)	Romania	44.3439	26.0123	110	bsrn	0.99	10.05	15.93
Carpentras	France	44.083	5.059	100	bsrn	1.86	7.34	11.70
Cener	Spain	42.816	-1.601	471	bsrn	-1.03	9.48	15.22
Eastern North Atlantic	Azores	39.0911	-28.0292	15.2	bsrn	1.20	10.64	16.48
Plataforma Solar de Almería	Spain	37.0909	-2.3581	500	iea pvps	-0.22	6.39	11.17
Oujda	Morocco	34.65	-1.9	618	enermena	1.35	6.95	11.01
Tataouine	Tunisia	32.974	10.485	210	iea pvps	-4.71	8.75	12.79
Tataouine	Tunisia	32.92967	10.45177	276	enermena	-0.16	6.83	10.65
Missour	Morocco	32.86	-4.107	1043	enermena	1.04	6.65	11.22
Ghardaia	Algeria	32.386	3.78	463	iea pvps	-3.47	8.31	12.24
Erfoud	Morocco	31.49099922	-4.217999935	859	enermena	1.25	7.87	11.38
Sede Boqer	Israel	30.8597	34.7794	500	bsrn	1.15	5.54	9.02
Zagora	Morocco	30.27199936	-5.852000237	783	enermena	-2.01	7.45	11.89
Ma'an	Jordania	30.172	35.818	1012	iea pvps	-2.12	4.98	7.89
Cairo	Egypt	30.036	31.009	86	enermena	-3.08	6.99	10.38
Tan-Tan	Morocco	28.498	-11.322	56	enermena	-3.63	8.24	12.16
Izana	Tenerife, Spain	28.3093	-16.4993	2372.9	bsrn	-4.11	9.32	18.12
Tamanrasset	Algeria	22.7903	5.5292	1385	bsrn	-0.13	6.75	11.49
Paramaribo	Surinam	5.806	-55.2146	4	bsrn	7.64	18.63	26.87
Natal	South Africa	-5.8367	-35.2064	58	iea pvps	2.18	8.80	12.64
Caico	Brazil	-6.4669	-37.0847	165	inpe	-0.90	9.54	14.29
Dar Es Salaam	Tanzania	-6.78	39.2	122	iea pvps	0.89	13.76	21.33
Petrolina	Brazil	-9.068	-40.319	387	bsrn	2.68	10.18	15.30
Kasama	Zambia	-10.17165	31.22558	1392	esmap	3.61	11.55	16.21
Kasama	Zambia	-10.17165	31.22558	1381	iea pvps	3.52	11.53	16.19
Mutanda	Zambia	-12.423	26.215	1313	esmap	3.85	12.23	17.30
Mutanda	Zambia	-12.423	26.215	1318	iea pvps	3.90	12.25	17.31
Kasungu	Malawi	-13.0153	33.4684	1067	iea pvps	-1.28	11.72	18.55
Kaoma	Zambia	-14.839	24.931	1139	esmap	3.80	11.16	16.05

Name	Country	latitude (°)	longitude (°)	altitude (m)	Network	Mean Bias Error MBE (%)	Mean Absolute Error MAE (%)	Root Mean Square Error RMSE (%)
Kaoma	Zambia	-14.839	24.931	1172	iea pvps	4.07	11.23	16.11
Lusaka	Zambia	-15.39463	28.33722	1264	iea pvps	4.00	10.91	15.93
Chilanga	Zambia	-15.5483	28.24817	1221	esmap	5.01	12.25	17.48
Chilanga	Zambia	-15.5483	28.24817	1226	iea pvps	5.05	12.26	17.49
Brasilia	Brazil	-15.601	-47.713	1023	bsrn	3.16	14.00	22.12
Choma	Zambia	-16.83828	27.07046	1265	esmap	4.31	11.68	16.95
Choma	Zambia	-16.83828	27.07046	1284	iea pvps	4.43	11.73	16.98
Reunion Island University	Reunion, France	-20.9014	55.4836	116	bsrn	-3.15	15.61	24.22
Namibian University of Science and Technology	South Africa	-22.56500053	17.07500076	1683	sauran	5.75	8.95	13.41
Cachoeira Paulista	Brazil	-22.6896	-45.0062	574	iea pvps	2.02	12.81	20.96
Gobabeb	Namibia	-23.5614	15.042	407	bsrn	-4.42	6.99	9.86
CSIR Energy Centre	South Africa	-25.746519	28.278739	1400	sauran	1.01	6.70	10.98
Uni. Pretoria	South Africa	-25.7531	28.2286	1374	iea pvps	0.48	6.44	10.65
Florianopolis	Brazil	-27.6047	-48.5227	11	bsrn	0.51	12.69	20.63
Richtersveld	South Africa	-28.5608	16.7615	134	iea pvps	-1.61	5.11	7.68
Sao Martinho da Serra	Brazil	-29.4428	-53.8231	489	bsrn	0.44	11.12	17.29
Uni.of KwaZulu-Natal Westville [Durban]	South Africa	-29.817	30.945	200	iea pvps	0.42	8.77	13.10
De Aar	South Africa	-30.6667	23.993	1287	bsrn	-0.14	4.76	8.13
Vanrhynsdorp	South Africa	-31.61747932	18.73834038	130	iea pvps	3.78	6.31	8.91
South African Astronomical Observatory	South Africa	-32.378	20.812	1761	iea pvps	0.76	4.17	7.10
Graaff-Reinet	South Africa	-32.48546982	24.58581924	660	sauran	-0.05	6.23	10.22
University of Fort Hare	South Africa	-32.78461075	26.84519958	540	sauran	1.26	6.94	11.02
Nelson Mandela University	South Africa	-34.0086	25.6653	24	iea pvps	2.32	8.52	12.10

## 5.1.2 GOES East

The statistics of Vaisala Xweather solar model 3 GHI at hourly time step compared to high quality measurements in the field of view of Meteosat 0° satellites are given in the next table:

Name	Country	latitude (°)	longitude (°)	altitude (m)	Network	Mean Bias Error MBE (%)	Mean Absolute Error MAE (%)	Root Mean Square Error RMSE (%)
Sioux Falls	USA	43.73	-96.62	473	bsrn	1.60	14.64	23.35
Rock Springs	USA	40.72	-77.9333	376	bsrn	-0.19	13.22	20.15
Bondville	USA	40.0667	-88.3667	213	bsrn	1.08	11.13	19.17
Solar Technology Acceleration Center (SolarTAC)	USA	39.7569	-104.6203	1674	iea pvps	-0.73	12.79	21.07
Langley Research Center	USA	37.1038	-76.3872	3	bsrn	0.83	7.50	11.94
Billings	USA	36.605	-97.516	317	bsrn	-0.12	7.92	12.44
Southern Great Plains	USA	36.605	-97.485	318	bsrn	-1.38	8.34	13.15
Goodwin Creek	USA	34.2547	-89.8729	98	bsrn	1.59	9.37	14.74
University of Texas Pan-American Solar Radiation Lab (UTPA)	USA	26.3059	-98.1716	45.4	iea pvps	3.51	11.78	20.60
Selegua	Mexico	15.784	-91.9902	602	bsrn	2.58	8.68	13.75
Paramaribo	Surinam	5.806	-55.2146	4	bsrn	1.71	13.18	18.94
Natal	Brazil	-5.8367	-35.2064	58	iea pvps	2.44	10.26	14.16
Observatory of Huancayo	Peru	-12.05	-75.32	3314	bsrn	3.02	11.20	17.56
Brasilia	Brazil	-15.601	-47.713	1023	bsrn	0.85	15.69	23.86
Cachoeira Paulista	Brazil	-22.6896	-45.0062	574	iea pvps	0.99	11.58	17.71
Florianopolis	Brazil	-27.6047	-48.5227	11	bsrn	1.07	10.52	17.02

## 5.1.3 GOES West

The statistics of Vaisala Xweather solar model 3 GHI at hourly time step compared to high quality measurements in the field of view of GOES 15 (GOES West) satellite are given in the next table:

Name	Country	latitude (°)	longitude (°)	altitude (m)	Network	Mean Bias Error MBE (%)	Mean Absolute Error MAE (%)	Root Mean Square Error RMSE (%)
University of Oregon (SRML)	USA	44.0467	-123.0743	133.8	iea pvps	4.35	9.63	13.50
Boulder	USA	40.125	-105.237	1689	bsrn	0.20	12.99	20.50
Solar Technology Acceleration Center (SolarTAC)	USA	39.7569	-104.6203	1674	iea pvps	-2.64	10.73	18.57
Golden	USA	39.742	-105.18	1829	iea pvps	-0.66	12.57	19.92
Desert Rock	USA	36.626	-116.018	1007	bsrn	2.53	5.90	9.90
University of Nevada - Las Vegas	USA	36.107	-115.1425	615	iea pvps	-1.44	5.45	9.21
SOLRMAP Loyola Marymount University (RSR)	USA	33.9667	-118.4226	27	iea pvps	0.56	3.78	5.86
SOLRMAP University of Arizona (OASIS)	USA	32.2297	-110.9553	786	iea pvps	-0.02	5.48	9.68

## 5.2 Acronyms

<b>AOD</b>	Aerosol Optical Depth at 550 nm. This is one of atmospheric parameters computed by CAMS IFS model and used in McClear and Heliosat-V models.
<b>CAMS</b>	Copernicus Atmospheric Monitoring Service – meteorological model operated by the European service ECMWF (European Centre for Medium-Range Weather Forecasts)
<b>CSP</b>	Concentrated solar power systems, which use mirrors or lenses to concentrate sunlight onto a small area, where it is converted to heat, then to electricity.
<b>DIF</b>	Diffuse Horizontal Irradiation.
<b>DNI</b>	Direct Normal Irradiation.
<b>ECMWF</b>	European Centre for Medium-Range Weather Forecasts provides operational medium- and extended- range forecasts and a computing facility for scientific research.
<b>EUMETSAT</b>	European Organization for the Exploitation of Meteorological Satellites
<b>GHI</b>	Global Horizontal Irradiation.
<b>GOES</b>	Geostationary Operational Environmental Satellites operated by NOAA
<b>GTI</b>	Global Tilted Irradiation.
<b>Himawari</b>	Geostationary weather satellites operated by the Japanese Meteorological Agency (JMA)
<b>IODC</b>	Indian Ocean Data Coverage satellites operated by EUMETSAT
<b>JMA</b>	Japan Meteorological Agency
<b>MFG</b>	Meteosat First Generation satellites operated by EUMETSAT.
<b>MSG</b>	Meteosat Second Generation satellites operated by EUMETSAT.
<b>MTG</b>	Meteosat Third Generation satellites operated by EUMETSAT.
<b>NASA</b>	National Aeronautics and Space Administration
<b>NOAA</b>	National Oceanic and Atmospheric Administration
<b>PV</b>	Photovoltaic
<b>COP90</b>	Copernicus Digital Surface Model
<b>TMY</b>	Typical Meteorological Year

## 5.3 Glossary

Aerosols	Small solid or liquid particles suspended in air, for example clouds, haze, and air pollution such as smog or smoke.
All-sky irradiance	Solar radiation reaching the Earth's surface.
Mean Absolute Error (MAE)	Measures the average magnitude of the deviation between the ground station and the model $MAE = \frac{\sum_{i=1}^n  y_i - x_i }{n}$
Mean Bias Error (MBE)	Represents systematic deviation between the ground station and the model (positive bias indicates overestimation and negative bias shows underestimation of the model) $b = \frac{1}{N} \sum_{k=1}^N \delta_k$
Clear-sky irradiance	Solar radiation reaching the Earth's surface without taking into account the impact of clouds.
Time step	Period of aggregation of solar data that can be obtained from the Vaisala Xweather Solar Model 3
Root Mean Square Error (RMSE)	Represents spread of deviations between the ground station and the model $RMSE = \sqrt{\frac{1}{N} \sum_{k=1}^N \delta_k^2}$
Solar irradiance	Solar power (instantaneous energy) falling on a unit area per unit time [W/m <sup>2</sup> ].
Solar irradiation	Amount of solar energy falling on a unit area over a stated time interval [Wh/m <sup>2</sup> or kWh/m <sup>2</sup> ].

## 5.4 References

Blanc, P. and Wald, L.: The SG2 algorithm for a fast and accurate computation of the position of the Sun for multi-decadal time period, *Solar Energy*, 86, 3072–3083, <https://doi.org/10.1016/j.solener.2012.07.018>, 2012.

Driesse, A., Jensen, A., Perez, R., 2024. A Continuous form of the Perez diffuse sky model for forward and reverse transposition. *Solar Energy* vol. 267

D. G. Erbs, S. A. Klein and J. A. Duffie, Estimation of the diffuse radiation fraction for hourly, daily and monthly-average global radiation, *Solar Energy* 28(4), pp 293–302, 1982. Eq. 1

Emde, C., Buras-Schnell, R., Kylling, A., Mayer, B., Gasteiger, J., Hamann, U., Kylling, J., Richter, B., Pause, C., Dowling, T., and Bugliaro, L.: The libRadtran software package for radiative transfer calculations (version 2.0.1), *Geoscientific Model Development*, 9, 1647–1672, <https://doi.org/10.5194/gmd-9-1647-2016>, 2016.

Gschwind, B., Wald, L., Blanc, P., Lefevre, M., Schroedter-Homscheidt, M., and Arola, A.: Improving the McClear model estimating the downwelling solar radiation at ground level in cloud-free conditions - McClear-v3, *Meteorologische Zeitschrift*, 28, 147–163, <https://doi.org/10.1127/metz/2019/0946>, 2019.

Inness, A., Ades, M., Agustí-Panareda, A., Barré, J., Benedictow, A., Blechschmidt, A.-M., Dominguez, J. J., Engelen, R., Eskes, H., Flemming, J., Huijnen, V., Jones, L., Kipling, Z., Massart, S., Parrington, M., Peuch, V.-H., Razinger, M., Remy, S., Schulz, M., and Suttie, M.: The CAMS reanalysis of atmospheric composition, *Atmos. Chem. Phys.*, 19, 3515–3556, <https://doi.org/10.5194/acp-19-3515-2019>, 2019.

Qu, Z., Oumbe, A., Blanc, P., Espinar, B., Gesell, G., Gschwind, B., Klüser, L., Lefèvre, M., Saboret, L., Schroedter-Homscheidt, M., and Wald, L.: Fast radiative transfer parameterisation for assessing the surface solar irradiance: The Heliosat-4 method, *Meteorologische Zeitschrift*, 26, 33–57, <https://doi.org/10.1127/metz/2016/0781>, 2017.

Wanner, W., Strahler, A., Hu, B., Lewis, P., Muller, J.-P., Li, X., Schaaf, C., and Barnsley, M.: Global retrieval of bidirectional reflectance and albedo over land from EOS MODIS and MISR data: Theory and algorithm, *Journal of Geophysical Research D: Atmospheres*, 102, 17 143–17 161, <https://doi.org/10.1029/96JD03295>, 1997.

Tournadre, Benoît & Gschwind, Benoît & Saint-Drenan, Yves-Marie & Blanc, Philippe. (2021). An improved cloud index for estimating downwelling surface solar irradiance from various satellite imagers in the framework of a Heliosat-V method. [10.5194/amt-2020-480](https://doi.org/10.5194/amt-2020-480).

WMO: World Meteorological Organization Guide to Meteorological Instruments and Methods of Observation (updated 2017), Chapter 7: Measurement of radiation, WMO, 2014.

Xie, Y., Sengupta, M., and Dudhia, J.: A Fast All-sky Radiation Model for Solar applications (FARMS): Algorithm and performance evaluation, *Solar Energy*, 135, 435–445, <https://doi.org/10.1016/j.solener.2016.06.003>, 2016.

# Get in touch

Get in touch with our team to learn more about Xweather's solutions for renewable energy:

Rupam Chakraborti

Head of Product - Renewable Energy

[rupam.chakraborti@vaisala.com](mailto:rupam.chakraborti@vaisala.com)

